Characterizing Uncertainty in Upstream Regulation Actions for Operational Ensemble Streamflow Prediction

(NOAA/NWS/OHD; CFDA: 11:462 Hydrologic Research)

First Progress Report

By

Konstantine P. Georgakakos
Hydrologic Research Center, San Diego, CA 92130

and

Aris P. Georgakakos and **Huaming Yao**
Georgia Water Resources Institute and Georgia Tech, Atlanta, GA 30332

Award No. NA08NWS4620023

31 December 2008

1.0 Introduction

Operational hydrologic forecast models simulate the physical rainfall-runoff processes that underlay watershed outflow. Most watersheds, however, include storage and other distributed regulation facilities that modify the natural flow regime and introduce forecast discrepancies. In watersheds with large reservoirs or sizable known basin withdrawals and transfers, this problem can best be addressed by explicit modeling of the regulation process. In watersheds where regulation is the cumulative effect of small but many individual facilities, however, explicit regulation modeling is not practical. The purpose of the "Upstream Regulation" project is to develop and test procedures that (**1**) can incorporate the second type of watershed regulation in operational hydrologic forecasts, and (**2**) quantify the associated uncertainty. Quantifying the associated uncertainty enables reliable risk assessments, but it also provides the information to answer the question, "What approach should be used at a particular watershed: pure hydrologic modeling, explicit upstream regulation modeling, or implicit upstream regulation modeling?" Clearly, the answer to this question depends on whether the uncertainty size associated with each approach is operationally adequate.

The work reported herein investigates the potential to incorporate upstream regulation through the use of (**1**) Neural Networks or (**2**) Linear Regression models. These methods are investigated first because they can represent linear and nonlinear relationships, are robust and simple to implement, and can easily be packaged as part of operational forecasts. The methods are developed and tested for three watersheds of the American River at daily, weekly, and monthly time resolutions, and yield promising results. However, detailed assessments are continuing to determine the methods' operational adequacy and the need to consider other approaches.

This report includes 7 sections and two appendices. In Section 2, the three case study watersheds are briefly described including the available data and the origin of the hydrologic model simulations used in this work. Section 3 elaborates on the technical details of the methods used. Sections 4 and 5 discuss model calibration and testing, and Section 6 summarizes the important findings and continuing investigations. References are included in Section 7. Appendices A and B include tables and figures with additional details on calibration parameters and verification results.

2.0 Case Study Watersheds and Hydrologic Forecasts

The three forks (North, Middle and South Fork) of the American River drain approximately 4,800 km^2 of the mountainous terrain of central California (with elevations up to 3,000 m) and join to provide inflow to Folsom Lake (Figure 1). The catchment with outlet at Folsom Lake is characterized by typical orographic rainfall patterns associated with steep terrain barriers, and with snow in the high elevations (typically above 1500 m). The climatological means of hourly precipitation, based on a sample of precipitation events for the wet period 1980-1987, show a maximum of about 2 mm/hr over the headwaters of the North Fork of the American River with pronounced variability. The automated operational gauge network provides estimates of the mean areal precipitation that are nearly unbiased for the entire inflow watershed, but which

possess non-negligible bias for the Fork sub-catchments (*Tsintikidis et al. 2002*). The catchment average response time to significant rainfall events in the absence of snow is approximately 12 hours. Of particular interest for this work is the fact that significant and diverse upstream regulation is documented for the Middle and South Forks of the American River. Available data from the operational files of the California Nevada River Forecast Center (CNRFC) of the U.S. National Weather Service consist of: six-hourly mean areal precipitation and temperature for sub-catchments of the basin, monthly climatologies of daily potential evapotranspiration demand for each sub-catchment, and observed mean daily streamflow for all the Forks and reconstructed Folsom Lake inflow from Lake levels.

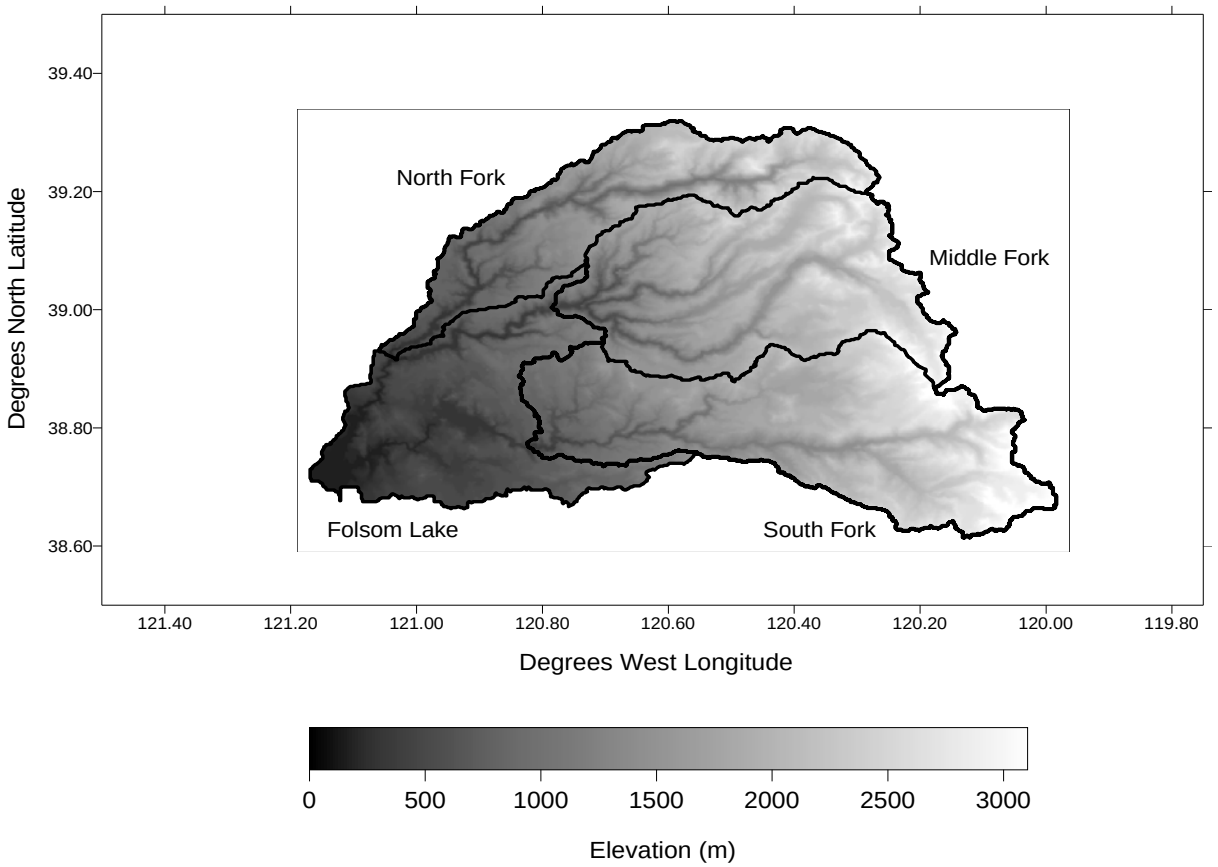

Figure 1: Folsom Lake catchment and the sub-catchments of the North, Middle and South Forks of the American River.

The hydrologic model used in this study to generate flow simulations and forecasts contains important features of the CNRFC operational hydrologic model, including the components for snow accumulation and ablation, soil water accounting, and channel routing. These components of the stand alone hydrologic model were designed and implemented to mirror the analogous components of the operational CNRFC forecast model. It is an adaptation of the operational model as it includes distributed channel routing in order to more accurately reproduce the timing

of the flows throughout the stream network. The model consists of adaptations of the operational snow accumulation and ablation model (*Anderson 1973*) and the Sacramento soil water accounting model as described in *Georgakakos (1986)*. For channel routing, the kinematic channel routing model of *Georgakakos and Bras (1982)* is used in the form of a sequence of linear conceptual reservoirs, with parameters estimated from the CNRFC estimates of unit hydrographs applied to the sub-catchments of interest (see *Sperfslage and Georgakakos 1996* for a description of the procedure).

The hydrologic basin upstream of the Folsom Lake reservoir was subdivided into sub-basins considering stream gauge sites, significant upstream reservoir facilities, available automated precipitation and temperature sensors, and the topology of the channel network. Those sub-basins, which have significant elevation differences within their areas, are further subdivided into sub-areas (an upper and a lower sub-area in this version of the stand alone model). The snow and the soil-water models are applied to each of the sub-areas to produce rain plus melt and channel inflow volumes, respectively. These volumes are then fed into the channel routing model and are carried downstream through the channel network undergoing time distribution, advection and attenuation. The model produces outflow at all the gauging sites and all the junctions of the model-channel network, and, of course, at the basin outlet (inflow point into the reservoir). It is important to note that the stand-alone model is designed to use the same input as the operational hydrologic forecast model, and its parameters bear close relationship to the parameters of the operational hydrologic model. The values of the model parameters used by the operational model for the snow and soil-water components were used in the stand alone model as well, while (as mentioned earlier) a calibration process with available data was used to determine parameters for the channel routing model.

The configuration of the stand-alone model elements is exemplified for the Folsom Lake drainage in Figure 2. The North (NF), Middle (MF) and South (SF) Fork sub-basins are shown, sub-divided into an upper and a lower sub-area for snow-pack, soil-water accounting and channel routing. Channel routing occurs in each sub-area of each sub-basin and at channel network junctions the inflows are summed. Channel routing is indicated with red arrows in the Figure. There are four streamflow observation sites in the basin, shown with black filled circles. Of these, the one corresponding to the inflow point to Folsom Lake reports lake levels, which are transformed to naturalized flows. The model used also performs channel routing to the junctions without observations (open circles) to allow for the correct reproduction of the observed hydrograph with a six-hour temporal resolution.

The kinematic channel routing component of the stand alone model for each channel segment is based on a series of linear reservoirs with identical parameters. The sum of the inverse of the channel routing model parameters for all the reservoirs representing a single channel segment is equal to the travel time in the channel segment. The operational model uses unit hydrographs to reproduce channel processes. For the North, Middle and South Fork sub-basins, initial estimates of the parameters of the channel routing component of the stand-alone model were obtained by fitting the linear reservoir model to the appropriate unit hydrographs (e.g., see *Sperfslage and Georgakakos 1996* for numerical fitting procedure). Initial values of the parameters of the channel segments downstream of the Forks were based on preliminary estimates of the travel time in these segments based on drainage area size. Table 1 shows the parameter values of the

snow, soil and channel components of the stand alone hydrologic model for the Folsom Lake drainage sub-basins. The nomenclature of Table 2 is used. Table 3 shows the long-term-averaged daily values of evapotranspiration demand by month (adopted from the operational parametric input files of CNRFC) used by the model for the present numerical experiments.

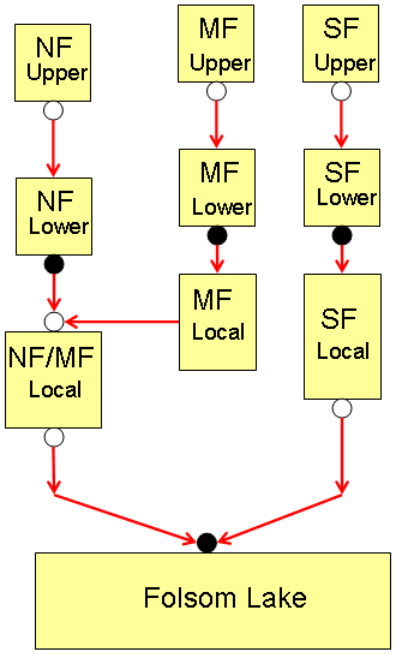

Figure 2: Representation of Folsom Lake drainage by the hydrologic prediction model. Sub-basins for which snow-pack and soil-water accounting is done are shown in yellow shade with sub-divisions into upper and lower sub-areas as appropriate. Routing segments are shown with red arrows, while junctions are shown with circles (filled black circles indicate gauged sites).

Table 1: Nominal Values of Stand Alone Model Parameters*

SNOW PARAMETERS

	NFu	*NFl*	*MFu*	*MFl*	*SFu*	*SFl*	*FL*
SCA	1.0	1.0	1.35	1.0	1.2	1.0	1.0
MFMAX	0.86	0.85	0.69	0.5	0.75	0.85	0.8
MFMIN	0.2	0.3	0.12	0.16	0.2	0.25	0.25
NMF	0.15	0.15	0.15	0.15	0.15	0.15	0.15
PLWHC	0.04	0.04	0.04	0.04	0.04	0.04	0.04
TIPM	0.25	0.25	0.25	0.25	0.25	0.25	0.25
MBASE	1.0	1.0	1.0	1.0	1.0	1.0	0.0
UADJ	0.04	0.04	0.04	0.04	0.08	0.06	0.04
DAYGM	0.1	0.1	0.1	0.1	0.1	0.1	0.1
PXTEMP	2.0	2.0	2.0	2.0	2.0	2.0	1.0
SI	900.	300.	1200.	600.	1100.	500.	200.
ELV	19.86	9.60	19.81	13.72	20.29	5.90	4.57
PADJ	1.0	1.0	1.0	1.0	1.1	1.05	0.97

SACRAMENTO MODEL PARAMETERS

	NFu	*NFl*	*MFu*	*MFl*	*SFu*	*SFl*	*Fl*
UZTWM	142.000	161.000	90.000	140.000	100.000	175.000	75.000
UZFWM	55.000	35.000	35.000	45.000	65.000	90.000	15.000
LZTWM	312.000	360.000	270.000	280.000	250.000	600.000	180.000
LZFPM	72.000	72.000	96.000	110.000	125.000	350.000	100.000
LZFSM	110.000	85.000	120.000	110.000	20.000	60.000	80.000
DU	0.075	0.070	0.105	0.115	0.040	0.050	0.062
DLPR	0.001	0.002	0.001	0.002	0.001	0.001	0.001
DLDPR	0.018	0.030	0.023	0.015	0.007	0.007	0.018
EPS	20.000	20.000	48.000	43.000	30.000	100.000	12.000
THSM	1.400	1.400	1.300	1.500	2.100	1.100	1.200
PF	0.250	0.350	0.150	0.300	0.250	0.250	0.250
XMIOU	0.000	0.000	0.000	0.000	0.000	0.000	0.100
ADIMP	0.010	0.010	0.000	0.020	0.000	0.000	0.075
PCTIM	0.000	0.000	0.005	0.005	0.000	0.000	0.065
ETADJ	1.000	1.000	1.000	1.000	1.000	1.000	1.000

KINEMATIC CHANNEL ROUTING MODEL INITIAL PARAMETERS

	NFu	*NFl*	*MFu*	*MFl*	*SFu*	*SFl*	*MF-NF*	*MF/NF-F*	*SF-F*
n_c	1	2	1	2	3	1	2	2	2
α	5.40	0.85	4.40	0.95	4.40	0.80	4.0	4.0	0.95

SUB-CATCHMENT AREAS (km²)

	NFu	*NFl*	*MFu*	*MFl*	*SFu*	*SFl*	*Fl*
Area	325.1	550.4	713.0	533.5	898.6	632.3	1016.3

*See Table 2 for nomenclature used in this Table

Table 2: Nomenclature for Table 1

HEADINGS

For Snow, Sacramento Models, Channel Routing Model and for Areas
NFu: NORTH FORK UPPER SUB-AREA
NFl: NORTH FORK LOWER SUB-AREA
MFu: MIDDLE FORK UPPER SUB-AREA
MFl: MIDDLE FORK LOWER SUB-AREA
SFu: SOUTH FORK UPPER SUB-AREA
SFl: SOUTH FORK LOWER SUB-AREA
Fl: FOLSOM LAKE LOCAL SUB-BASIN

For Channel Routing Model
MF-NF: CHANNEL SEGMENT CONNECTING THE OUTLET OF MIDDLE FORK WITH A JUNCTION POINT DOWNSTREAM OF THE NORTH FORK OUTLET
NF/MF-F: CHANNEL SEGMENT THAT CONNECTS THE JUNCTION POINT DOWNSTREAM OF NORTH FORK OUTLET WITH FOLSOM LAKE INFLOW POINT
SF-F: CHANNEL SEGMENT THAT CONNECTS THE OUTLET OF SOUTH FORK WITH FOLSOM LAKE INFLOW POINT

SNOW MODEL PARAMETERS

SCA: SNOW CATCH ADJUSTMENT FACTOR
MFMAX: MAXIMUM MELT FACTOR (MM $DEGC^{-1}$ D^{-1})
MFMIN: MINIMUM MELT FACTOR (MM $DEGC^{-1}$ D^{-1})
NMF: MAXIMUM NEGATIVE MELT FACTOR (MME $DEGC^{-1}$ D^{-1})
PLWHC: FRACTION OF SNOW COVER FOR WATER HOLDING SNOW CAPACITY
TIPM: PARAMETER FOR ANTECEDENT TEMPERATURE INDEX COMPUTATIONS
MBASE: BASE TEMPERATURE FOR MELT COMPUTATIONS (DEGC)
UADJ: AVERAGE DAILY WIND FUNCTION FOR RAIN-ON-SNOW PERIODS (MM MB^{-1} DAY^{-1})
DAYGM: CONSTANT MELT AT SNOW-SOIL INTERFACE (MM DAY^{-1})
PXTEMP: TEMPERATURE TO DELINEATE RAIN FROM SNOW (DEGC)
SI: MAXIMUM SWE FOR 100% COVER IN SNOW DEPLETION CURVE (MM)
ELV: ELEVATION OF CENTROID OF BASIN (10^2 M)
PADJ: PRECIPITATION ADJUSTMENT FACTOR

SACRAMENTO MODEL PARAMETERS

UZTWM: UPPER ZONE TENSION WATER CAPACITY (MM)
UZFWM: UPPER ZONE FREE WATER CAPACITY (MM)
LZTWM: LOWER ZONE TENSION WATER CAPACITY (MM)
LZFPM: LOWER ZONE FREE PRIMARY WATER CAPACITY (MM)
LZFSM: LOWER ZONE FREE SUPPLEMENTARY WATER CAPACITY (MM)
DU: INTERFLOW RECESSION ($6HRS^{-1}$)
DLPR: RECESSION COEFFICIENT FOR LOWER ZONE FREE PRIMARY WATER ELEMENT ($6HRS^{-1}$)
DLDPR: RECESSION COEFFICIENT FOR LOWER ZONE FREE SUPPLEMENTARY WATER ELEMENT ($6HRS^{-1}$)
EPS: CONSTANT FACTOR IN PERCOLATION FUNCTION
THSM: EXPONENT IN PERCOLATIOIN FUNCTION
PF: FRACTION OF PERCOLATION BYPASSING THE LOWER ZONE TENSION WATER ELEMENT
XMIOU: FRACTION OF WATER LOST TO DEEP GROUNDWATER LAYERS
ADIMP: ADDITIONAL IMPERVIOUS AREA MAXIMUM FRACTION
PCTIM: FRACTION OF PERMANENTLY IMPERVIOUS AREA
ETADJ: EVAPOTRANSPIRATION DEMAND ANNUAL ADJUSTMENT FACTOR

CHANNEL MODEL PARAMETERS

n_c: NUMBER OF LINEAR RESERVOIRS REPRESENTING THE CHANNEL SEGMENT UNDER STUDY
α: COMMON COEFFICIENT OF LINEAR RESERVOIRS WITH INVERSE DESCRIBING TRAVEL TIME ($6HRS^{-1}$)

Table 3: Daily Values of Evapotranspiration Demand Used by the Sacramento Model for Each Month (Values in mm/d)

	NFu	NFl	MFu	MFl	SFu	SFl	Fl
J	0.760	1.280	0.760	1.280	0.780	1.300	0.860
F	0.780	1.400	1.060	1.860	1.450	2.470	1.120
M	0.820	1.800	1.470	2.520	1.670	2.940	1.640
A	1.030	2.290	1.950	3.110	1.800	3.200	2.480
M	1.800	3.640	2.550	4.110	2.280	3.850	4.150
J	3.040	6.040	4.320	6.330	3.580	7.390	4.560
J	5.260	8.220	5.400	8.650	5.760	9.160	4.640
A	5.570	8.250	6.150	9.730	5.840	8.760	4.100
S	4.100	6.550	4.770	6.950	3.270	3.790	3.220
O	1.940	3.100	2.690	3.120	1.810	2.300	2.200
N	1.140	1.690	1.190	1.440	1.360	2.050	1.230
D	0.910	1.400	0.940	1.250	1.080	1.800	0.880

3.0 Implicit Upstream Regulation Methods

3.1 Artificial Neural Networks

Artificial neural network models were first introduced in the field of speech and image recognition to mimic human-like brain functions. These models are composed of many nonlinear computational elements operating in parallel and arranged in patterns resembling biological neural nets. Computational elements or nodes are connected via weights that are adapted with use to improve performance. Neural networks have found applications in many fields for learning to simulate various input-output processes from sets of observed data.

A neural network consists of two basic elements: nodes and arcs connecting different nodes. A real number called weight is usually assigned to each arc. The **weight** w_{ij} specifies the strength of information that node i receives from node j. Each node (also called processing unit) receives information from other nodes or externally, and produces an output after passing all its inputs through an **activation function** associated with it. A node receiving input from outside is called input node. A node is called output node if its output is one of the network outputs; otherwise, it is called a hidden node.

Various configurations and layouts of neural networks have been constructed for solving particular problems. The layered feedforward network is used widely and is easy to implement. In this work, it is used as the basic neural network structure. The layered feedforward network arranges its nodes into different layers. The bottom layer contains the input nodes. The top layer contains the output nodes. All nodes in the middle layers are hidden nodes. Connections exist only between nodes of adjacent layers. The input nodes receive external information and pass it on to the nodes of the first hidden layer through the weighed arcs which, in turn, propagate it further up until it reaches the nodes of the output (top) layer. In the layered feedforward network, the information propagates from the bottom to the top. A typical layered feedforward network is depicted in Figure 3.

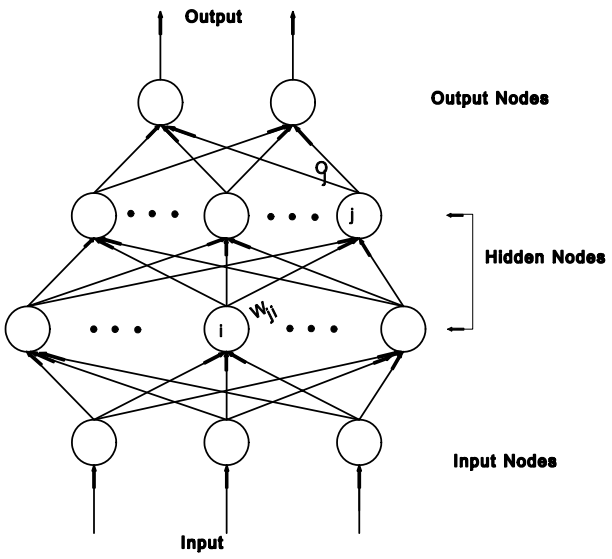

Figure 3: Typical Layered Feedforward Neural Network

A network with fixed weights and activation functions determines a relationship between inputs and outputs. This relationship can be simple or complicated depending on the network structure and the activation function forms. For a layered feedforward network, the activation functions play a crucial role in identifying the correct relations. In this respect, sigmoidal functions have been shown to perform very well as activation functions. Sigmoidal functions tend to 1 at positive infinity and 0 at negative infinity. It has been shown that *any* continuous function can be uniformly approximated by continuous sigmoidal functions. Other functions such as the hard limiter, threshold logic, and sigma-pi have also been used successfully in many fields. In this work, however, the sigmoidal function will be the basis of the activation NN function.

For a given neural network structure, the parameter estimation problem consists of determining the weights such that the network can best derive the input-output data relationship. This process is called “training” and uses measured input-output data pairs to find the "optimal weights". The training process begins with some initial weight estimates which are used to produce an output to certain inputs. This output is subsequently compared with the desired output of the training data set and the weights are adjusted to minimize the discrepancy. This procedure is repeated many times until weight convergence, and it can be fast or slow depending on the method used for weight adjustment. Many weight updating rules exist, including the Delta rule with weight updating after each input-output pair which has proved to be simple to implement and efficient with respect to convergence rate and computational requirements.

The Delta rule essentially implements a gradient descent procedure. The objective function for the training process is

$$E = \frac{1}{2} \text{Min} \sum_{p}^{N} \sum_{j}^{M} (t_{pj} - O_{pj})^2 ,$$

where N is the number of training data pairs, M is the output node number, t_{pj} is the desired value of the jth output node for input pattern p, and O_{pj} is the jth element of the actual output associated with input p. Every node except the input nodes on the first layer receives data from the nodes of previous layers. The total received by input node j is called the net of node j and is denoted by net_{pj}:

$$net_{pj} = \sum_i W_{ji} O_{pi} \ ,$$

where W_{ji} is the weight from node i of the previous layer to node j. Thus, the output of node j is given by:

$$O_{pj} = f_j(net_{pj}) \ .$$

The weight adjustment is based on the Delta rule after presenting each data pair, and it is given by:

$$\Delta_p W_{ji} = \eta \delta_{pj} O_{pi} \ ,$$

where η is called the learning rate, taking values between 0 and 1, and δ_{pj} is called the error term of node j and is given by:

$$\delta_{pj} = \begin{bmatrix} (t_{pj} - O_{pj}) f_j'(net_{pj}) & if \quad j \quad is \quad an \quad output \quad node \\ f_j'(net_{pj}) \sum_k \delta_{pk} W_{kj} & otherwise \end{bmatrix} .$$

The learning process involves two phases: During the first phase, the input is presented and propagated forward through the network to compute the output value O_{pj}. This output is then compared with the desired value t_{pj}, resulting in an error ε_{pj} for each output node. The second phase involves a backward pass through the network during which the error is passed to each node and the appropriate weight changes are made.

The above weight updating rule is called the generalized Delta rule for the multilayer feedforward network. The larger the learning rate is, the larger are the changes of the weights.

3.2 Regression Models

Linear regression models are used in this work as a more parsimonious alternative to the NN models, and are developed using the same input data.

4.0 Model Calibration and Testing

4.1 Neural Network (NN) Models

The NN model is used to establish the relationship between the unimpaired flow forecasts (of the hydrologic model) and the observed (regulated) flows. NN models are developed for the

North, Middle, and South Fork watersheds, draining into the Folsom reservoir on the American river. Flow measurements are available at the exit of each watershed. Several small storage reservoirs exist in the Middle and South Fork watersheds, while the North Fork watershed is largely undeveloped.

The daily sequences of observed and simulated flows at each site are plotted in the Figures of Appendix B. The flow correspondence is generally good. The two sequences follow similar patterns and are correlated well. The error statistics and correlation coefficients at different time resolutions are summarized in Table 4. The Middle Fork watershed is subsequently used as a test-bed for additional tests and its results are reported first.

Table 4: Hydrologic Model Statistics

		Error Mean (cfs)	Error StD (cfs)	Correlation Coef
Daily	**Middle Fork**	-105.41	1096.74	0.87
	North Fork	23.64	521.40	0.96
	South Fork	252.29	1144.36	0.82
Weekly	**Middle Fork**	-105.40	930.41	0.86
	North Fork	23.64	360.28	0.98
	South Fork	252.67	940.70	0.84
Monthly	**Middle Fork**	-104.95	783.84	0.84
	North Fork	23.31	240.26	0.98
	South Fork	253.47	728.34	0.86

The development of the NN models proceeds as follows: The data record of each site is divided into three segments used for NN training (first 50% of the record), calibration (middle 30% of the record), and validation (last 20% of the record). The training segment is used to train the NN model parameters. After each training cycle, the NN model is applied to the calibration data set, and the error statistics are computed. The NN training process is stopped when the simulation error in the calibration data set is minimized. The validation data set is used to assess the NN performance for data that have not been used in the NN development.

The activation function used for each node is

$$O_{pj} = f_j(net_{pj}) = \frac{1}{1 + exp\left\{-\left(\sum_i W_{ji} O_{pi} + \theta_j\right)\right\}}$$

where θ_j is a bias associated with node j and is learned (estimated) as all other NN weights. The sigmoidal function is continuous and differentiable everywhere.

The output range of the activation function is between zero and one. However, flows are not necessarily within this range. Thus, to utilize this function, appropriate data preprocessing is required. To satisfy the requirement, the following linear transformation is used to bring the data into the zero-one range:

$$Q' = A\frac{Q_{max} - Q}{Q_{max} - Q_{min}} + B\frac{Q - Q_{min}}{Q_{max} - Q_{min}} .$$

The above expression is a general linear transformation in which Q is the original flow value, Q' is the transformed value, Q_{max}, Q_{min} are the maximum and minimum values of the entire series, and A and B are the lower and upper bounds after the transformation. It is noted that the activation function cannot take the values 1 and 0 without infinitely large weights, implying that the network will never produce Q_{max} and Q_{min}. One way to resolve this problem is to let A be higher than 0 and B lower than 1. A and B are part of NN model parameters. The NN model output should be transferred back to the original scale using the inverse transformation.

Several NN structures were tested in this study against several criteria to be presented later in the section. A structure with five input nodes and one hidden layer with five hidden nodes was found to perform best for all sites at daily and weekly time resolutions, while a simpler NN structure is more suitable at the monthly time resolution because of limited data availability. In what follows, this NN structure is used for all time resolutions to assess the forecast improvements at the daily and weekly time scales and highlight the dependence of NN performance to data availability at the monthly time scale.

The NN input nodes consist of three previous observed flows, O(k-1), O(k-2), and O(k-3); the current unimpaired flow forecast, I(k); and the previous unimpaired flow forecast, I(k-1). Here k represents the current time period. The optimal NN structure is shown below:

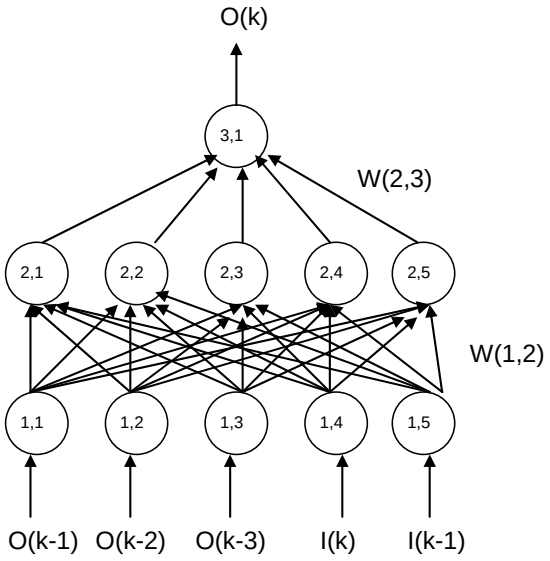

Figure 4: Optimal NN Structure

The training process requires 2,000 to 6,000 iterations to converge for all NN models. These computations take less than a minute on a ThinkPad T61 notebook computer. When training

is complete, the optimal model parameters are saved (Tables A.1 through A.9 in Appendix A). Simulations are then carried out using the optimal NN models to assess their performance. Error statistics (mean and standard deviation) and correlation coefficients between observed and modeled flows are computed separately for the training, calibration, and validation data sets. These results are reported in Tables 5, 6, and 7 for the daily, weekly, and monthly time resolutions respectively. For comparison, these tables also include the same statistics for the hydrologic forecasts and the regression models. Error statistics were developed for many alternative model forms, both NN and regression type. The models described herein are selected based on their performance against the above-mentioned statistics.

The NN models show significant improvement over the original hydrologic forecasts as indicated by the higher correlations between observed and simulated data and the smaller error standard deviations.

For the Middle Fork watershed at daily resolution, compared to the hydrologic model forecasts, the NN results generally exhibit smaller bias, smaller error standard deviation, and higher correlation with observed data. More specifically, the calibration and validation period biases of the hydrologic model are reduced from -87 and -198 cfs respectively to -59 and -25 cfs; the calibration and validation period error standard deviations are reduced from 1067 and 1051 cfs respectively to 791 and 659 cfs (a 30 to 40% reduction); and the calibration and validation correlation coefficients with observed data are increased from 0.89 and 0.92 respectively to 0.94 and 0.96. Similar results (a 33% standard deviation reduction) are obtained for the weekly time resolution, while the monthly improvements are marginal (Table 6 and 7). The relative decline of the NN performance at the monthly time scale is due to limited data availability introducing biases in the NN parameters. In this regard, the NN models can achieve better performance by using a simpler network structure, as discussed below.

For the largely undeveloped North Fork watershed, the hydrologic model forecasts are substantially better than those for the other two watersheds, and the use of the NN model yields small forecast improvements.

Lastly, for the South Fork watershed, the NN forecast improvements (over the hydrologic model performance) are comparable to those of the Middle Fork watershed for the daily and weekly time resolutions. The performance at the monthly time scale is not as good, highlighting the need for a simpler NN structure with fewer parameters. In this respect, based on the results reported herein, it is recommended that the number of data points per NN parameter in the training data set be higher than 20 to 25. This is the number of data points corresponding to the weekly NN implementation, while the monthly NN implementation only affords five data points per parameter.

The time series comparisons between the observed and simulated data are plotted in Figures B.1 through B.12 in Appendix B.

4.2 Regression Models

The following linear regression model form was found to perform best for all sites and time resolutions:

$$O(k) = A_1 O(k-1) + A_2 O(k-2) + A_3 O(k-3) + A_4 I(k) + A_5 I(k-1) + A_6 \ ,$$

where k is the time index, O is the output variable (observed flow), I is the input variable (unimpaired flow forecast from the hydrologic model), and A_i , i=1, 2, …, 6, are regression coefficients.

For consistency with the NN model calibration process, the regression parameters are estimated using the training data set (Table A.10 in Appendix A). The model is then applied to the calibration and validation data sets to assess its error characteristics. These statistics are listed in Tables 5, 6, and 7, and the corresponding sequences are plotted in Figures B.13 through B.21 in Appendix B.

For the Middle and South Fork watersheds, the regression models show significant improvements over the hydrologic model in terms of zero biases, smaller error standard deviations, and higher correlation coefficients with observed data. As in the NN models, the forecast improvements for the North Fork watershed are small. The *overall* performance of the regression models (with respect to the stated criteria) is comparable and occasionally slightly better than that of the NN models. The next section investigates these performance gains and differences in more detail and clarifies from where they accrue.

5.0 Performance Analysis by Flow Range

The performance comparisons of the previous section are based on error bias, error standard deviation, and correlation coefficient between forecasted and observed data *over the entire data range*. However, upstream regulation is expected to exert different flow impacts on different ranges of the flow frequency distribution, with such impacts expected to be more pronounced in medium to low flows than in high flows. Thus, to determine which model performs best, it is useful to quantify model performance over different distribution ranges.

Toward this goal, the Middle Fork watershed results are re-analyzed over three different flow ranges corresponding to the lower quartile, the middle half, and the upper quartile of the observed frequency distribution. For the training data set, the corresponding flow ranges are 35 to 330 cfs, 331 to 1340 cfs, and 1341 to 65000 cfs respectively. The flow ranges for the calibration and validation data sets are similar.

Performance statistics are computed as in the previous section for each frequency distribution range, and comparative data plots are generated separately for the training, calibration, and validation data sets. In addition, the range frequency distributions of the observed data, hydrologic model forecasts, NN model forecasts, and regression model forecasts are also plotted. All tables and figures are included in Appendix C. A summary of the results is compiled on Table 8.

Examination of the validation period results reveal significant model performance differences noted below.

- As expected, the hydrologic model performs best in the upper frequency quartile, where natural, unimpaired flow conditions dominate. In that range, its correlation coefficient with the observed flows is 0.92. Its performance, however, declines considerably in the other two frequency ranges with the correlation coefficient dropping to 0.46 and 0.41 respectively in the middle half and the lower frequency quartile. This is clearly observed in Figure C.3.2 (middle half), where the impact of flow regulation in smoothing out the natural inflow hydrographs is evident. The same comment applies for the lower quartile (dry conditions), although some performance improvement is noted during very dry and extended periods (with flows less than 200 cfs), where upstream storage is totally depleted. These observations are corroborated by the frequency distribution graphs where frequency distribution discrepancies between hydrologic model forecasts and observed flows are seen clearly.

- After post-processing by the NN or the regression models, the hydrologic forecasts correspond considerably better with the observed flows for all frequency ranges. The most notable improvement occurs with post-processing using the NN approach for the middle half frequency range. There, the correlation coefficient of the original hydrologic model forecasts increases from 0.46 to 0.84, the error standard deviation decreases from 584 cfs to 147 cfs, and the error bias decreases from 119 cfs to -24 cfs. Improvements are also noted using the regression model, but they are clearly inferior to those of the NN. This is seen on Figure C.3.2 where (1) the regression results experience frequent downward departures from the observed flows, and (2) the NN frequency distribution corresponds exceptionally well with that of the observed flows. Figure C.3.1 indicates that the regression model discrepancies increase in the lower quartile, with the NN maintaining better correspondence with the observed flows.

This analysis shows that the NN performs better than the regression model, more so than the assessment of Section 4 initially indicated. The reason for this is attributed to the NN ability to represent the nonlinear response that characterizes the flow modification in different flow frequency ranges. This ability of the NN approach resides in its nonlinear activation functions and larger parameter set. In this respect, the regression approach may improve if different regression models are calibrated for different frequency ranges. This and other possible improvements are currently being investigated.

6.0 Conclusions

The purpose of this study is to develop mathematical models to correct for upstream regulation impacts on hydrologic flow forecasts. The models investigated here are based on neural networks and linear multiple regression. These methods are investigated first because they can represent linear and nonlinear relationships, are robust and simple to implement, and can easily be packaged as part of operational forecasts. The models were developed and tested for three watersheds in the American River and were shown to realize significant advances toward estimating observed flows from unimpaired model-simulated flows in streams with upstream regulation. Detailed comparative analyses of model performance

demonstrated that the NN approach is able to represent the nonlinear flow modification more effectively across high, medium, and low flow frequency ranges, albeit at the expense of a larger parameter set.

In the next project phase, the NN and regression models will be refined further and tested in multi-lead forecasts. Improvements are expected if separate regression models are generated for different flow ranges, and if simpler NN structures are identified at the monthly time resolution where data availability is relatively limited. NN and regression model modifications designed to generate a better match across the entire frequency range will also be tested. With respect to multi-lead forecasts, the NN and regression models will be tested against several criteria to quantify their bias, accuracy, and reliability properties. As part of this investigation, procedures to characterize forecast uncertainty through forecast ensembles will also be developed.

Other, more physically based methods to incorporate upstream regulation may also be researched if the NN and regression models proved to be inadequate.

7.0 References

Anderson, E.A., 1973: National Weather Service River Forecast System – Snow accumulation and ablation model. *NOAA Technical Memorandum NWS HYDRO-17*. Office of Hydrology, National Weather Service, NOAA, Silver Spring, MD, 217pp.

Georgakakos, K. P., 1986: A Generalized stochastic hydrometeorological model for flood and flash-flood forecasting, 1 Formulation. *Water Resources Research* **22**(13), 2083-2095.

Georgakakos, K.P., and R.L. Bras, 1982: Real-time statistically linearized adaptive flood routing. *Water Resources Research* **18**(3), 513-524.

Sperfslage, J.A., and K.P. Georgakakos, 1996: Implementation and testing of the HFS operation as part of the National Weather Service River Forecast System (NWSRFS). *HRC Technical Report No. 1*. Hydrologic Research Center, San Diego, CA, 213pp.

Tsintikidis, D., Georgakakos, K.P., Sperfslage, J.A., Smith, D.E., and T.M. Carpenter, 2002: Precipitation Uncertainty and Raingauge Network Design within the Folsom Lake Watershed. *ASCE Journal of Hydrologic Engineering* **7**(2), 175-184.

Table 5: Daily Error Statistics

Site	Stats	Model Training Period			Calibration Period			Validation Period		
Middle Fork	Date Interval	10/1/1960-11/30/1979			12/1/1979-5/31/1991			6/1/1991-1/29/1999		
	Data Points	7000			4200			2800		
		Hydro Model	NN Model	Reg Model	Hydro Model	NN Model	Reg Model	Hydro Model	NN Model	Reg Model
	Error Mean	-76.65	-91.30	0.00	-87.36	-59.09	8.17	-198.06	-25.99	-5.16
	Error StDev	1134.55	481.40	636.89	1066.95	791.56	595.99	1051.20	658.99	629.38
	Corr. Coef	0.81	0.97	0.94	0.89	0.94	0.96	0.92	0.96	0.96
North Fork	Date Interval	10/1/1960-11/30/1979			12/1/1979-5/31/1991			6/1/1991-1/29/1999		
	Data Points	7000			4200			2800		
		Hydro Model	NN Model	Reg Model	Hydro Model	NN Model	Reg Model	Hydro Model	NN Model	Reg Model
	Error Mean	40.66	-24.53	-0.01	20.38	-32.22	-10.70	-18.73	-43.97	-29.37
	Error StDev	402.64	305.13	302.06	601.59	539.59	501.13	640.84	594.80	539.66
	Corr. Coef	0.97	0.98	0.98	0.96	0.97	0.97	0.95	0.96	0.97
South Fork	Date Interval	8/1/1964-2/7/1982			2/8/1984-8/13/1992			8/14/1992-8/17/1999		
	Data Points	6400			3840			2560		
		Hydro Model	NN Model	Reg Model	Hydro Model	NN Model	Reg Model	Hydro Model	NN Model	Reg Model
	Error Mean	279.71	-111.42	0.00	201.50	-121.73	-9.24	248.16	-102.20	32.76
	Error StDev	1105.60	481.58	546.84	1063.01	476.78	468.02	1343.38	935.59	604.31
	Corr. Coef	0.75	0.94	0.92	0.83	0.97	0.96	0.88	0.92	0.96

Table 6: Weekly Error Statistics

Site	Stats	Model Training Period			Calibration Period			Validation Period		
Middle Fork	Date Interval	10/2/1960-11/25/1979			12/02/1979-5/26/1991			6/2/1991-1/24/1999		
	Data Points	1000			600			400		
		Hydro Model	NN Model	Reg Model	Hydro Model	NN Model	Reg Model	Hydro Model	NN Model	Reg Model
	Error Mean	-76.67	-33.39	0.00	-87.09	49.06	15.43	-200.54	23.32	4.43
	Error StDev	971.70	374.07	610.99	899.19	610.91	631.29	876.96	587.26	590.67
	Corr. Coef	0.79	0.96	0.90	0.89	0.96	0.94	0.92	0.96	0.95
North Fork	Date Interval	10/2/1960-11/25/1979			12/02/1979-5/26/1991			6/2/1991-1/24/1999		
	Data Points	1000			600			400		
		Hydro Model	NN Model	Reg Model	Hydro Model	NN Model	Reg Model	Hydro Model	NN Model	Reg Model
	Error Mean	40.65	-36.51	0.00	20.42	-40.95	-12.38	-18.40	-63.45	-35.80
	Error StDev	308.28	270.80	232.23	394.97	380.87	336.31	418.33	379.50	391.25
	Corr. Coef	0.98	0.98	0.98	0.98	0.98	0.98	0.97	0.98	0.98
South Fork	Date Interval	8/2/1964-2/7/1982			2/14/1982-6/14/1992			6/21/1992-5/9/1999		
	Data Points	915			540			360		
		Hydro Model	NN Model	Reg Model	Hydro Model	NN Model	Reg Model	Hydro Model	NN Model	Reg Model
	Error Mean	280.96	-27.13	0.00	197.96	-9.62	-20.35	251.54	27.94	39.67
	Error StDev	917.64	428.27	563.73	938.17	538.62	599.50	1004.05	763.90	699.18
	Corr. Coef	0.78	0.94	0.89	0.84	0.95	0.93	0.89	0.92	0.94

Table 7: Monthly Error Statistics

Site	Stats	Model Training Period			Calibration Period			Validation Period		
Middle Fork	Date Interval	10/1/1960-11/1/1979			12/01/1979-5/1/1991			6/1/1991-1/1/1999		
	Data Points	230			138			92		
		Hydro Model	NN Model	Reg Model	Hydro Model	NN Model	Reg Model	Hydro Model	NN Model	Reg Model
	Error Mean	-75.34	87.26	0.00	-86.40	137.23	10.72	-200.06	116.65	-8.52
	Error StDev	820.25	392.58	563.10	748.20	631.45	588.71	751.06	567.12	492.27
	Corr. Coef	0.75	0.93	0.85	0.88	0.90	0.90	0.92	0.91	0.93
North Fork	Date Interval	10/1/1960-11/1/1979			12/01/1979-5/1/1991			6/1/1991-1/1/1999		
	Data Points	230			138			92		
		Hydro Model	NN Model	Reg Model	Hydro Model	NN Model	Reg Model	Hydro Model	NN Model	Reg Model
	Error Mean	40.28	13.22	0.00	21.09	12.42	-22.40	-20.32	-22.20	-59.97
	Error StDev	222.98	201.50	189.52	262.90	274.40	227.49	239.64	282.35	276.68
	Corr. Coef	0.98	0.98	0.98	0.98	0.98	0.98	0.98	0.98	0.98
South Fork	Date Interval	8/1/1964-1/1/1982			2/1/1982-7/1/1992			8/1/1992-7/1/1999		
	Data Points	210			126			84		
		Hydro Model	NN Model	Reg Model	Hydro Model	NN Model	Reg Model	Hydro Model	NN Model	Reg Model
	Error Mean	278.86	61.76	0.00	204.29	111.41	-48.75	244.69	264.90	85.49
	Error StDev	742.56	426.83	516.43	718.22	616.92	585.69	709.99	815.10	634.88
	Corr. Coef	0.79	0.91	0.87	0.87	0.92	0.91	0.91	0.89	0.93

Table 8: Model Performance Statistics by Frequency Range (Middle Fork; Daily Res.)

(a) Middle Fork Daily Performance Statistics for the Training Data Set

		Error Mean (cfs)	Error StD (cfs)	Correlation Coef
Lower Quartile	**Hydro Model**	-155.74	373.64	0.48
	Regression	-90.60	124.17	0.62
	NN	-72.13	77.58	0.58
Middle Half	**Hydro Model**	-22.12	884.28	0.16
	Regression	8.60	229.86	0.71
	NN	-54.25	177.88	0.76
Upper Quartile	**Hydro Model**	-85.30	1915.08	0.80
	Regression	95.26	1244.38	0.92
	NN	183.22	849.17	0.96

(b) Middle Fork Daily Performance Statistics for the Calibration Data Set

		Error Mean (cfs)	Error StD (cfs)	Correlation Coef
Lower Quartile	**Hydro Model**	-245.42	472.80	0.46
	Regression	-110.70	138.86	0.57
	NN	-61.32	80.73	0.56
Middle Half	**Hydro Model**	83.42	690.04	0.28
	Regression	21.07	194.89	0.76
	NN	-61.50	153.52	0.79
Upper Quartile	**Hydro Model**	-85.30	1915.08	0.80
	Regression	101.76	1110.68	0.95
	NN	248.18	1507.09	0.91

(c) Middle Fork Daily Performance Statistics for the Validation Data Set

		Error Mean (cfs)	Error StD (cfs)	Correlation Coef
Lower Quartile	**Hydro Model**	-204.35	433.70	0.41
	Regression	-120.93	176.97	0.49
	NN	-57.75	113.21	0.49
Middle Half	**Hydro Model**	119.64	584.48	0.46
	Regression	44.74	234.03	0.75
	NN	-24.11	147.44	0.84
Upper Quartile	**Hydro Model**	-826.70	1564.62	0.92
	Regression	11.62	1194.29	0.95
	NN	302.47	1210.72	0.96

Appendix A: Optimal NN and Regression Model Parameters

Table A.1: NN Parameter Values for Middle Fork Daily Model

Layer Number:	3				
Node Number:	5	5	1		
Weights:	-0.888884	-3.582958	-4.999488	0.914281	7.314926
	5.618609	7.500558	2.780233	1.524323	0.829251
	3.947812	8.040352	1.618159	3.376513	-0.318189
	-3.701609	-8.076194	-0.697389	4.847134	14.24186
	1.480669	4.244882	1.206704	2.707429	10.15535
	-3.658513				
	-7.44486				
	-3.823135				
	3.510368				
	12.13742				
Node Bias:	1.529248	2.681082	-1.509441	-3.208427	1.081049
	-3.692075				
WMAX0:	66471.1				
WMIN0:	35				
A0:	0.001				
B0:	0.999				

Table A.2: NN Parameter Values for North Fork Daily Model

Layer Number:	3				
Node Number:	5	5	1		
Weights:	-3.158966	-7.58816	-1.216348	4.48385	19.4596
	2.540033	3.89808	1.860423	0.309008	8.075477
	0.561392	0.704708	8.873977	0.027843	3.022941
	-2.105885	-6.06054	-1.361921	1.19585	16.97616
	-1.579313	-1.458238	4.325389	-0.340015	10.07345
	-3.89908				
	-7.330797				
	-4.864519				
	1.734884				
	13.20588				
Node Bias:	3.280693	-0.710318	1.890808	-2.305154	1.461949
	-6.325729				
WMAX0:	50100				
WMIN0:	0				
A0:	0.001				
B0:	0.999				

Table A.3: NN Parameter Values for South Fork Daily Model

Layer Number:	3				
Node Number:	5	5	1		
Weights:	-2.041518	-2.460196	-0.656964	1.792492	7.297321
	4.277334	8.341756	0.563343	3.133529	-0.339188
	0.212028	2.795342	-3.3074	0.900303	-1.616237
	-2.213365	-1.734348	-2.879643	2.551316	22.99903
	1.999793	5.020986	0.603094	-1.025133	7.20419
	-4.098245				
	-6.679822				
	-3.42211				
	3.881461				
	12.73089				
Node Bias:	2.133452	1.32463	-0.276076	-2.906683	1.073274
	-4.48808				
WMAX0:	83845.91				
WMIN0:	0.2				
A0:	0.001				
B0:	0.999				

Table A.4: NN Parameter Values for Middle Fork Weekly Model

Layer Number:	3				
Node Number:	5	5	1		
Weights:	-2.884821	-0.888122	-0.780764	2.585708	5.726822
	2.628122	8.308178	2.560712	2.287221	-0.435371
	0.541663	3.617836	0.585292	0.664613	-0.194924
	-0.068559	-0.176908	0.243502	2.633347	14.70384
	-0.537318	3.529567	-0.116316	0.896137	6.190801
	-3.354298				
	-7.638834				
	-1.626635				
	2.695825				
	11.41788				
Node Bias:	1.772357	1.08794	1.671737	-1.840379	0.676701
	-2.783616				
WMAX0:	28905.71				
WMIN0:	39.14286				
A0:	0.001				
B0:	0.999				

Table A.5: NN Parameter Values for North Fork Weekly Model

Layer Number:	3				
Node Number:	5	5	1		
Weights:	-3.080696	-2.684349	-0.949766	2.175233	16.85477
	2.027743	2.758696	2.181307	-0.035997	1.139837
	-0.564888	1.330233	1.080687	-0.226319	0.350007
	-0.740893	-2.397204	-1.130183	1.701647	4.992117
	-2.107294	0.528316	0.17924	0.302846	1.740648
	-4.63195				
	-5.008659				
	-3.177504				
	1.876221				
	10.09257				
Node Bias:	2.604283	-0.951954	0.614936	-1.627675	0.941672
	-4.76124				
WMAX0:	25204.29				
WMIN0:	12				
A0:	0.001				
B0:	0.999				

Table A.6: NN Parameter Values for South Fork Weekly Model

Layer Number:	3				
Node Number:	5	5	1		
Weights:	-0.823897	-3.156079	0.222071	0.688722	5.302401
	2.959521	6.223917	1.428093	0.854529	0.281573
	1.006442	4.502143	0.130396	0.928854	-0.843008
	0.138825	0.88944	-0.703542	2.175765	10.25612
	0.226638	3.865294	-0.099218	1.286337	4.479108
	-2.123748				
	-6.077235				
	-0.508851				
	2.910759				
	8.63878				
Node Bias:	2.460104	1.28883	0.717573	-1.484295	0.54942
	-3.13037				
WMAX0:	25757.92				
WMIN0:	21.42857				
A0:	0.001				
B0:	0.999				

Table A.7: NN Parameter Values for Middle Fork Monthly Model

Layer Number:	3				
Node Number:	5	5	1		
Weights:	-7.790933	-5.768942	4.261188	-0.639621	2.611355
	2.031633	4.867616	9.868016	9.055346	-3.358301
	2.936795	-0.314255	-4.883083	2.28842	2.501912
	1.430791	3.221581	2.021179	2.489327	11.3144
	-0.686704	10.47672	-3.033856	-10.77249	-2.34425
	-4.31511				
	-5.643095				
	-3.168276				
	2.379822				
	6.509402				
Node Bias:	-1.01274	2.822428	-1.435052	-1.604256	-0.43588
	0.501275				
WMAX0:	8874.73				
WMIN0:	42.76667				
A0:	0.001				
B0:	0.999				

Table A.8: NN Parameter Values for North Fork Monthly Model

Layer Number:	3				
Node Number:	5	5	1		
Weights:	-1.521528	-2.8502	-0.808751	2.908546	13.83522
	2.058204	0.478752	1.0185	-0.422062	-1.092726
	-0.284757	-0.208507	0.171692	1.192788	-0.759688
	2.211736	-1.736473	-0.16094	0.635577	2.854185
	-0.575878	1.789484	0.47564	0.724327	0.093654
	-3.282083				
	-3.819976				
	-1.569874				
	1.900481				
	8.79964				
Node Bias:	1.357093	2.239727	0.382052	-0.837071	0.824089
	-4.046144				
WMAX0:	8403.464				
WMIN0:	13.35484				
A0:	0.001				
B0:	0.999				

Table A.9: NN Parameter Values for South Fork Monthly Model

Layer Number:	3				
Node Number:	5	5	1		
Weights:	0.480401	-0.612357	-0.393393	3.128616	5.170573
	1.935438	3.443904	4.401286	-0.036534	3.495662
	0.368141	0.845927	0.960912	-0.792755	3.589649
	0.080935	-6.066286	2.335155	2.233803	7.048553
	0.856736	-0.078581	6.803391	0.53021	0.709168
	-0.44191				
	-3.704915				
	-4.721416				
	1.67848				
	5.888172				
Node Bias:	-0.709712	-0.941614	0.032526	-2.191775	-0.564498
	-2.162302				
WMAX0:	9672.581				
WMIN0:	41.75533				
A0:	0.001				
B0:	0.999				

Table A.10: Regression Model Parameters

	Sites	A1	A2	A3	A4	A5	A6	ErrMean	Err StDev
Daily	Middle Fork	0.856944	-0.688550	-0.014101	0.825331	-0.037666	50.489220	0.00	636.89
	North Fork	0.974699	-0.430458	-0.164625	0.494576	0.161898	-12.588500	-0.01	302.06
	South Fork	0.592255	-0.517824	0.048180	0.837042	-0.031868	134.766000	0.00	546.84
Weekly	Middle Fork	0.892717	-0.625552	-0.097315	0.585524	0.133095	107.403300	0.00	610.99
	North Fork	1.131627	-0.585203	-0.068850	0.518470	0.038052	-7.099128	0.00	232.23
	South Fork	0.657218	-0.392157	-0.092401	0.597608	0.131978	187.021200	0.00	563.73
Monthly	Middle Fork	0.702480	-0.561408	0.289821	0.654916	-0.299745	208.332200	0.00	563.10
	North Fork	1.155259	-0.370891	0.006100	0.240872	0.004796	5.111220	0.00	189.52
	South Fork	0.584500	-0.412246	0.159729	0.708328	-0.229759	365.004500	0.00	516.43

Appendix B: Figures of Observed vs. Modeled Flows

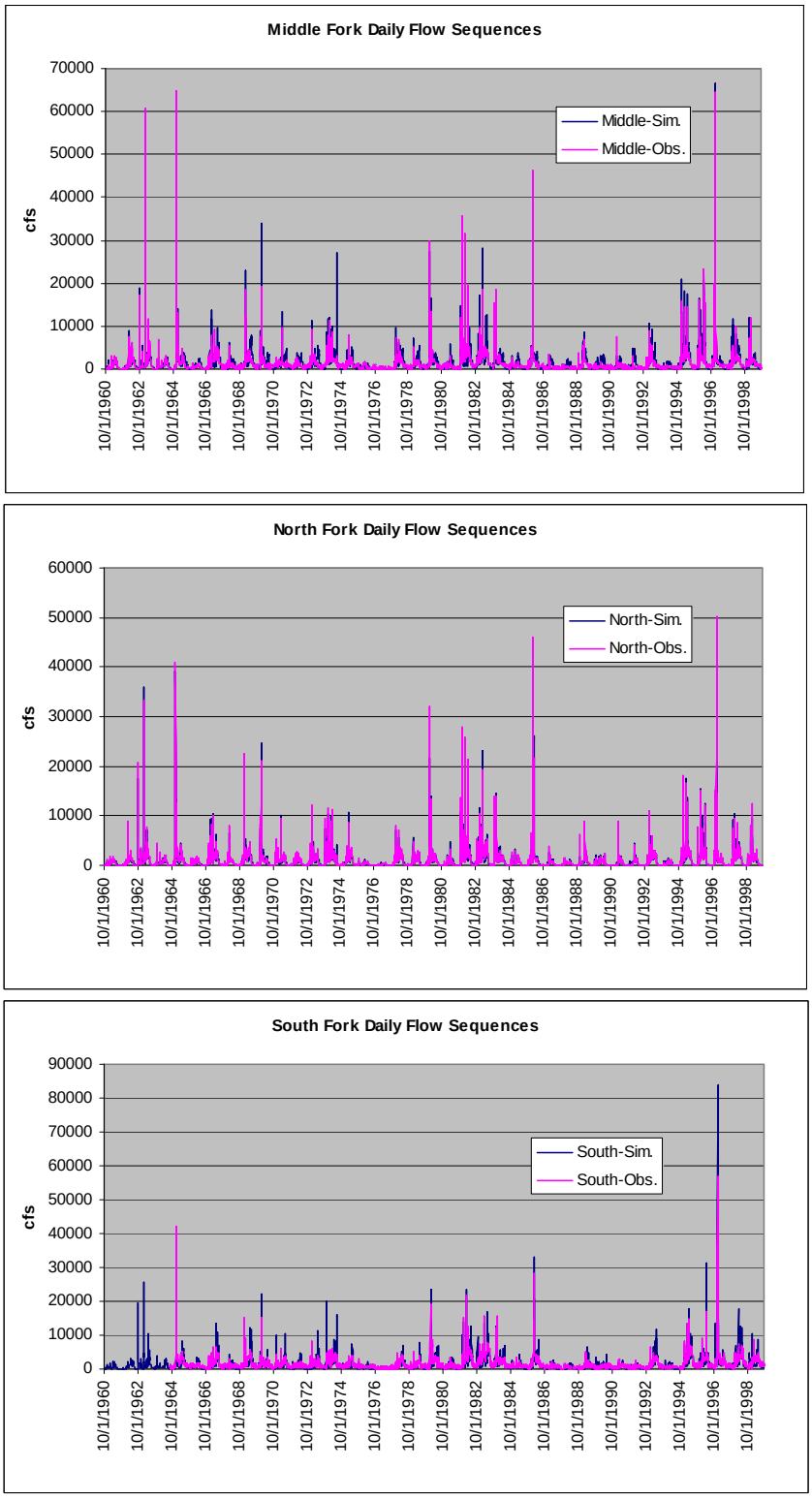

Figure B.1: Daily Flow Sequences

Figure B.2: Weekly Flow Sequences

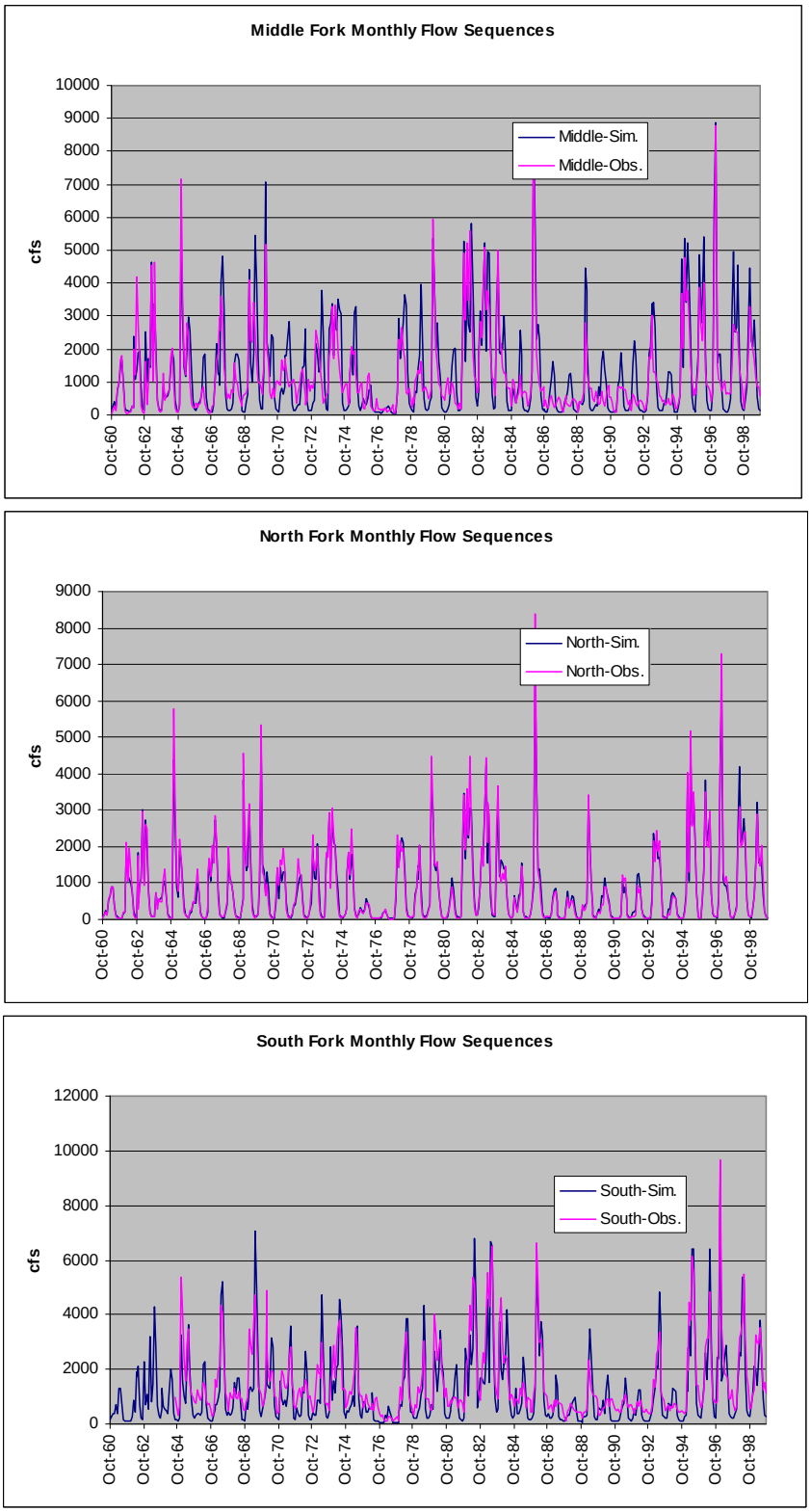

Figure B.3: Monthly Flow Sequences

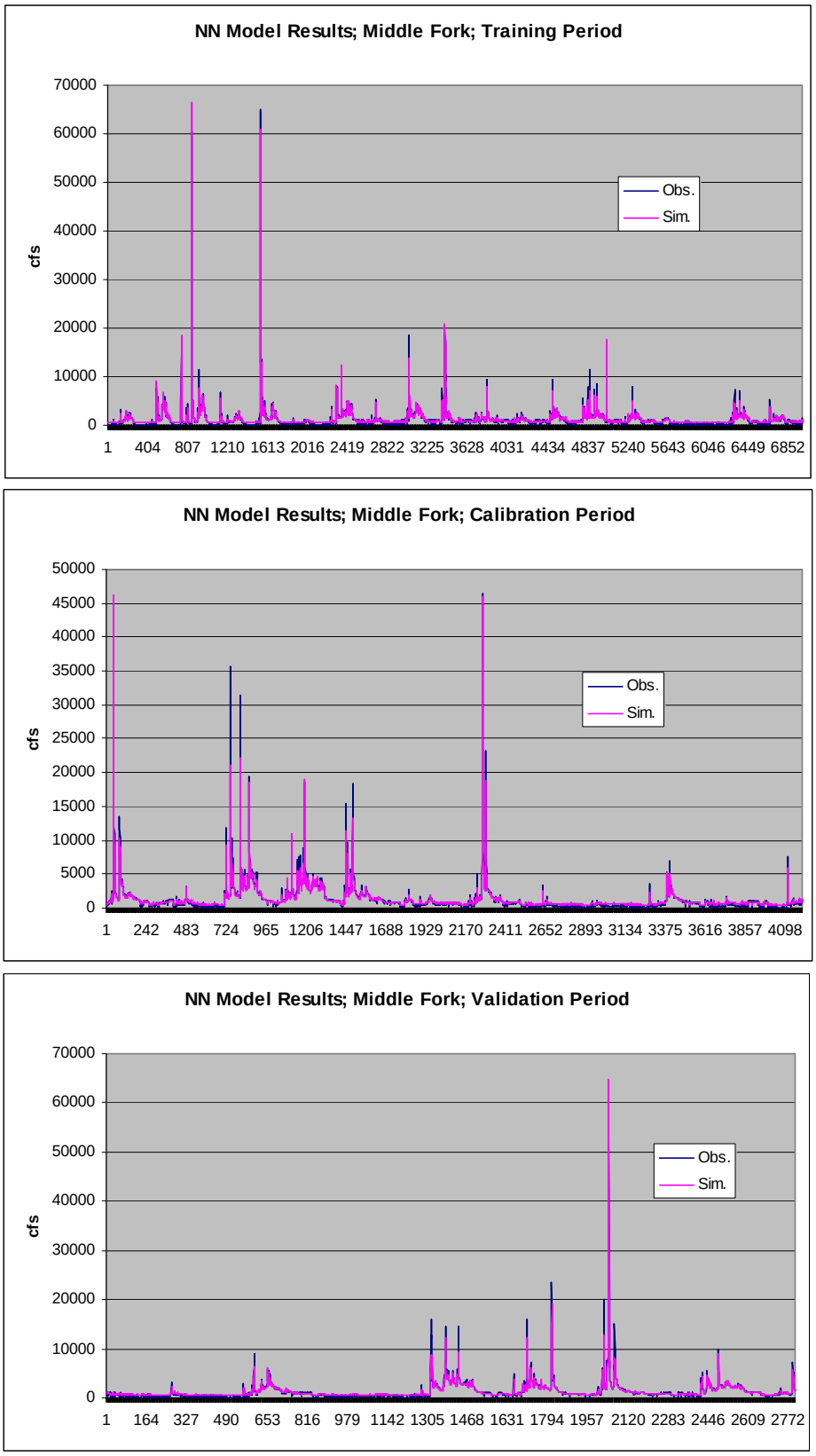

Figure B.4: Daily NN Model Results; Middle Fork;

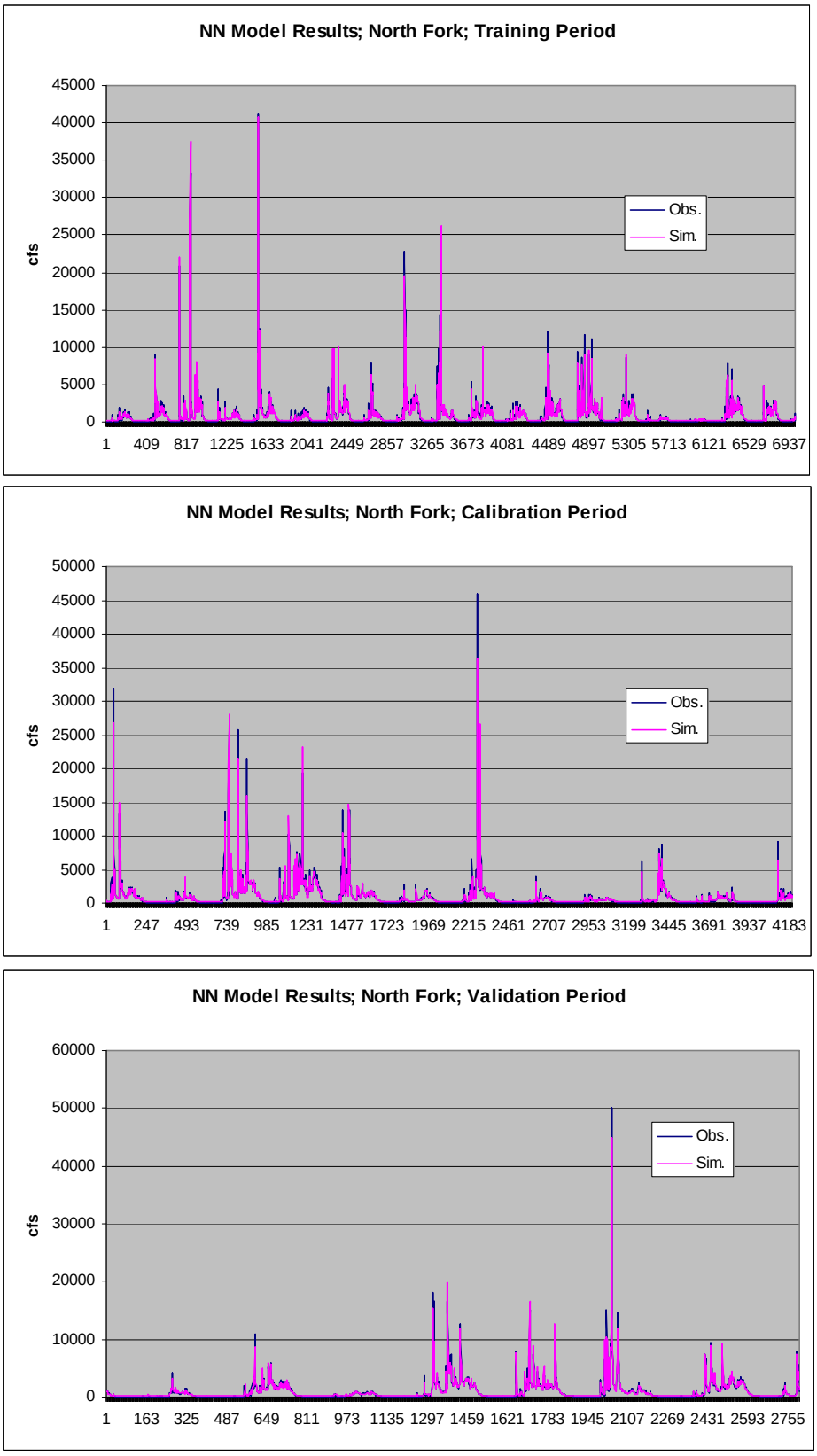

Figure B.5: Daily NN Model Results; North Fork

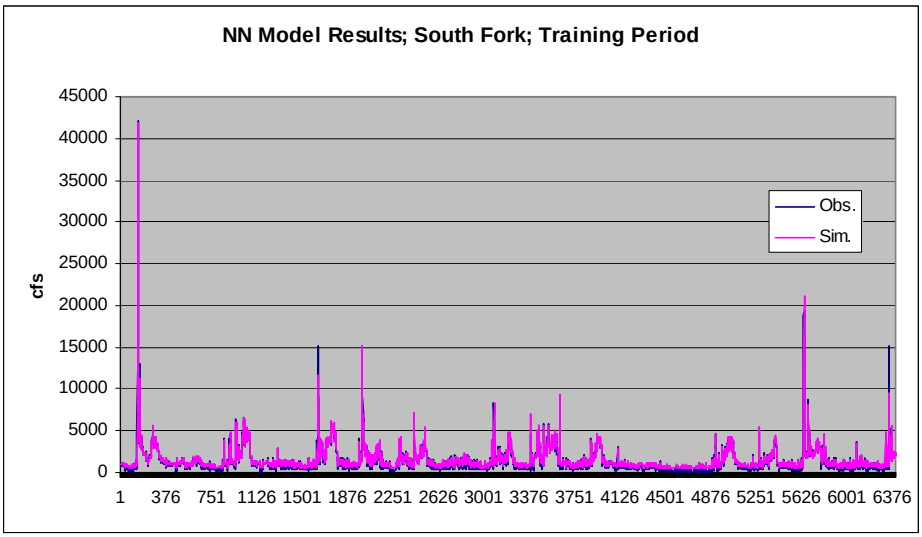

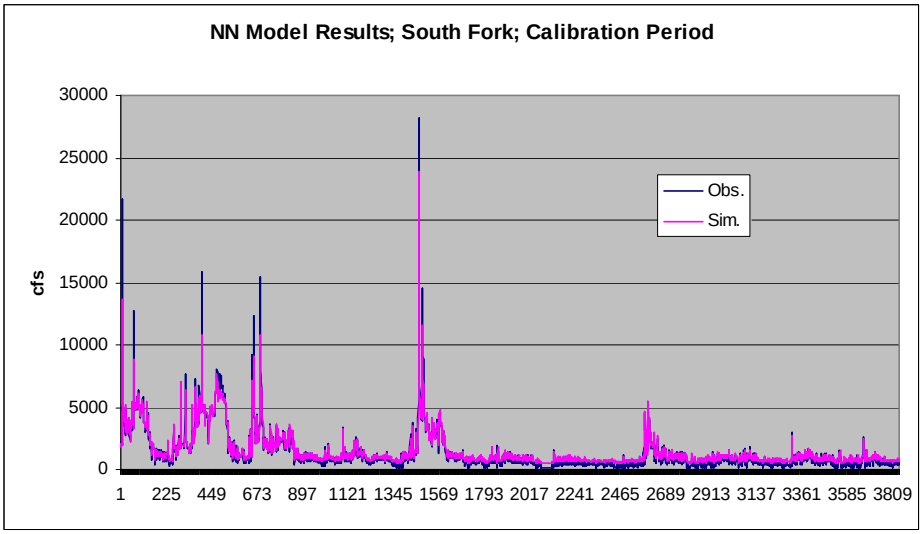

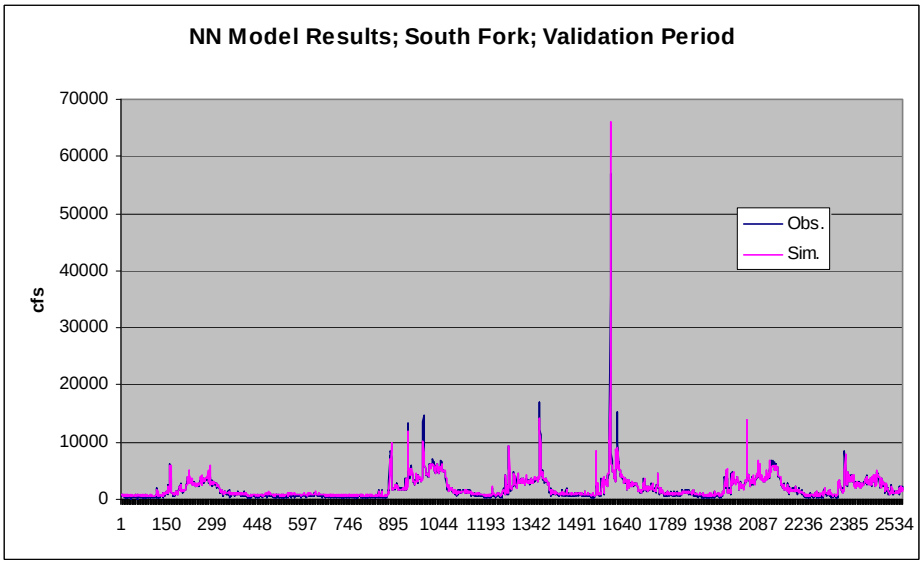

Figure B.6: Daily NN Model Results; South Fork

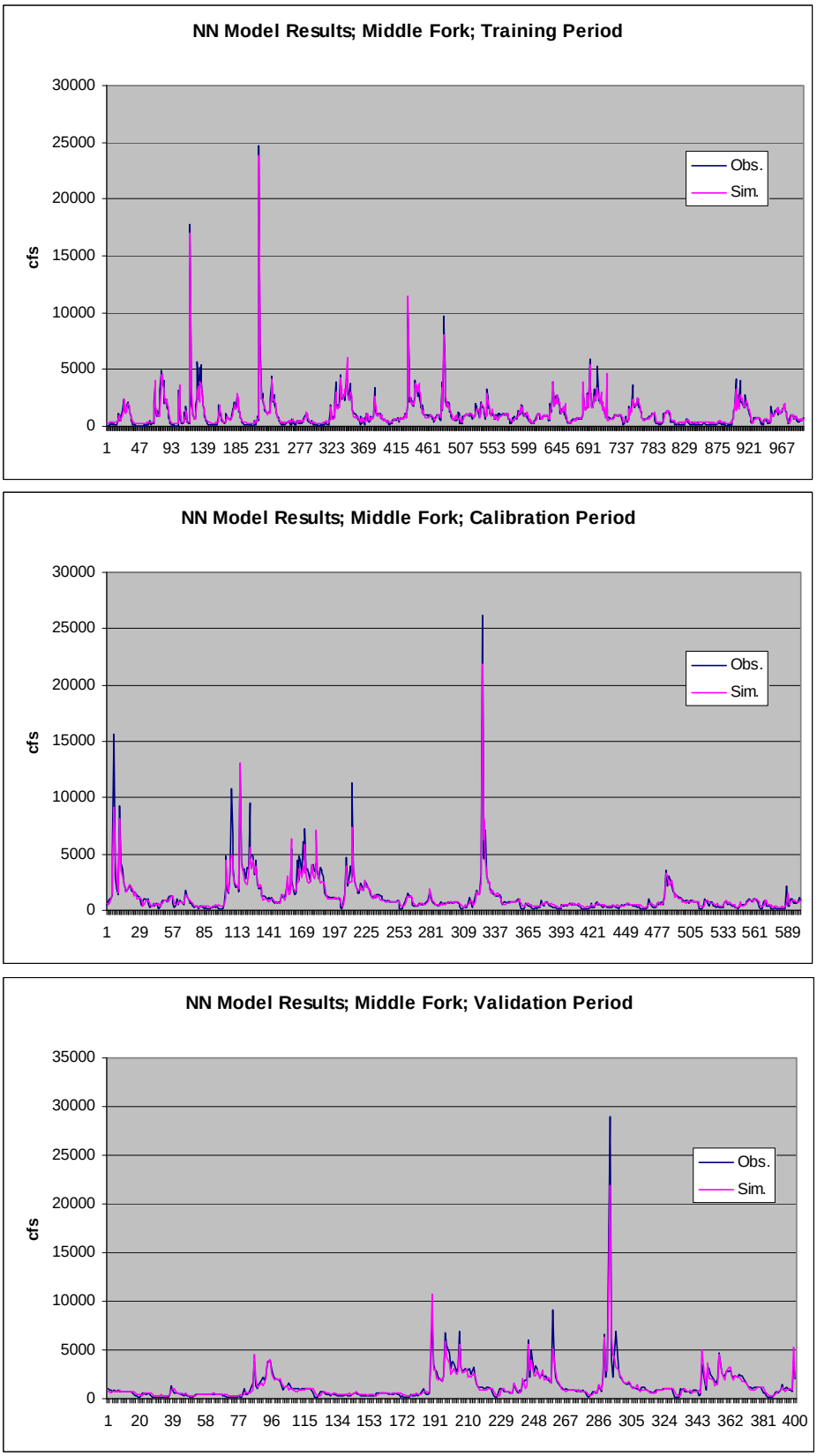

Figure B.7: Weekly NN Model Results; Middle Fork

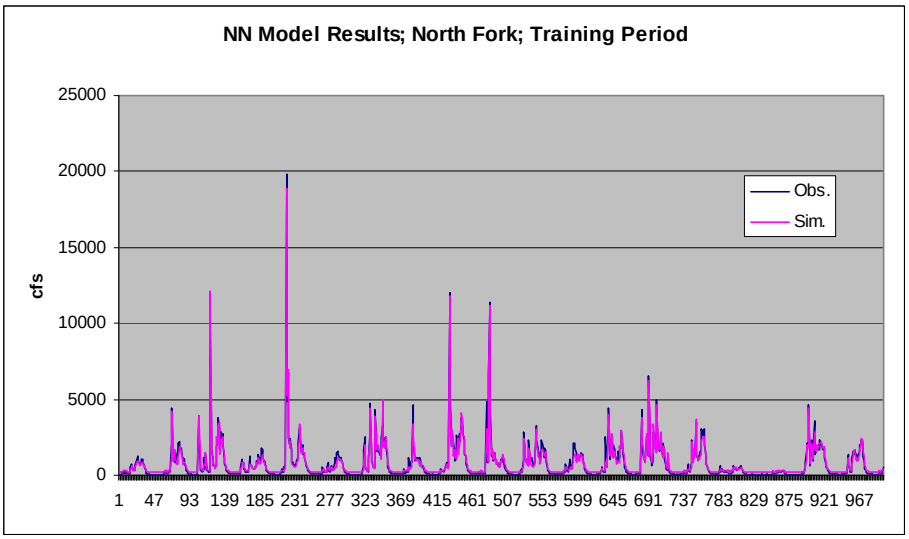

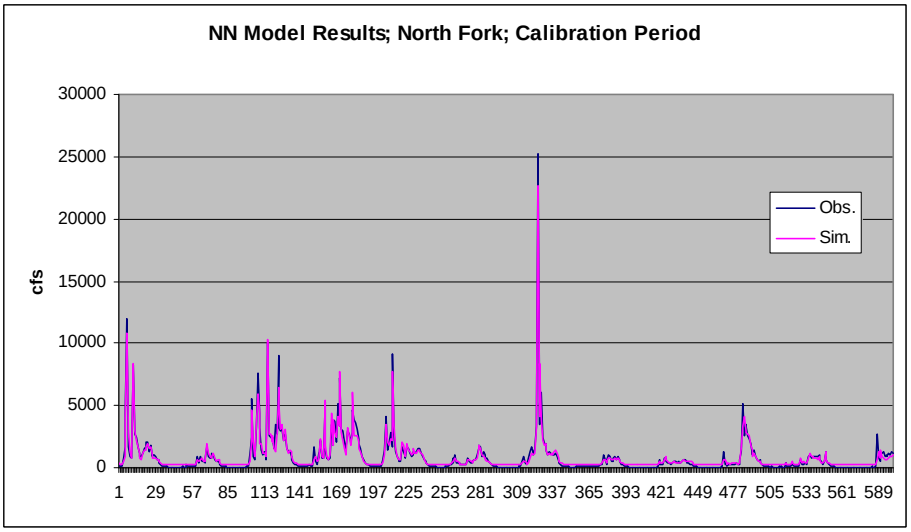

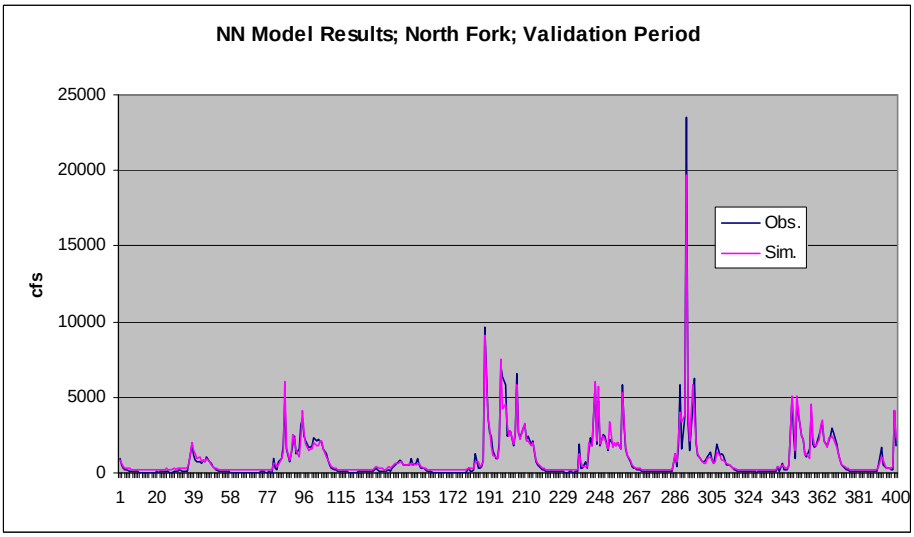

Figure B.8: Weekly NN Model Results; North Fork

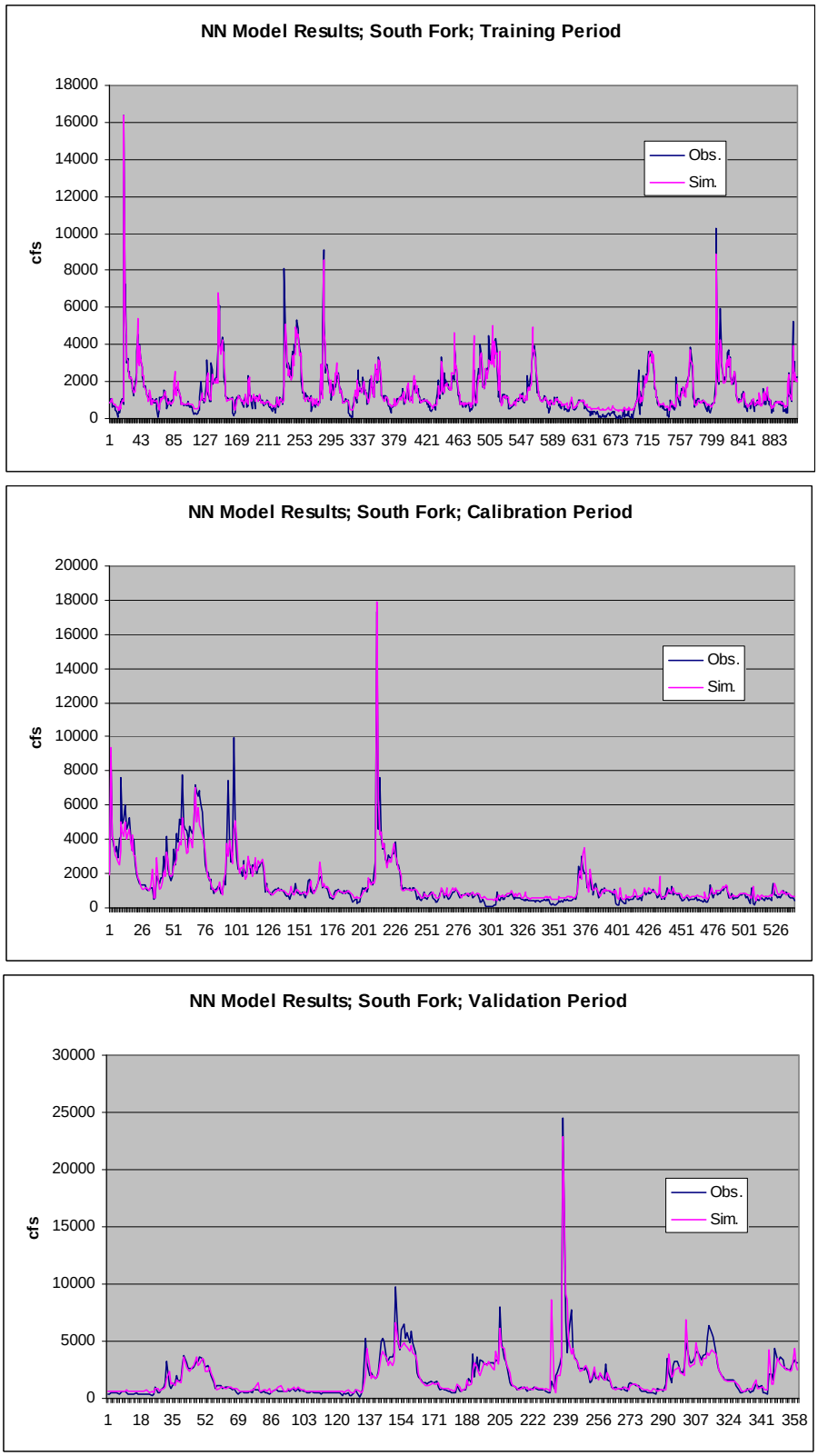

Figure B.9: Weekly NN Model Results; South Fork

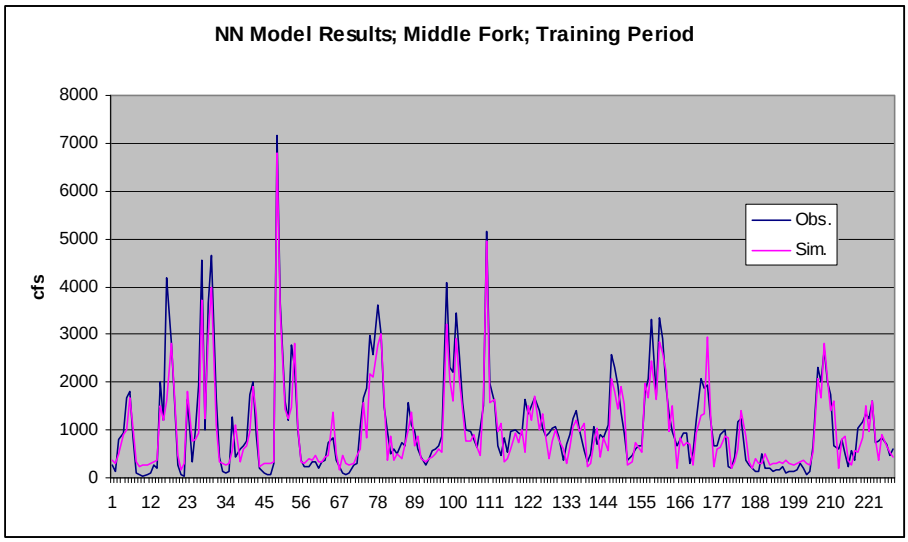

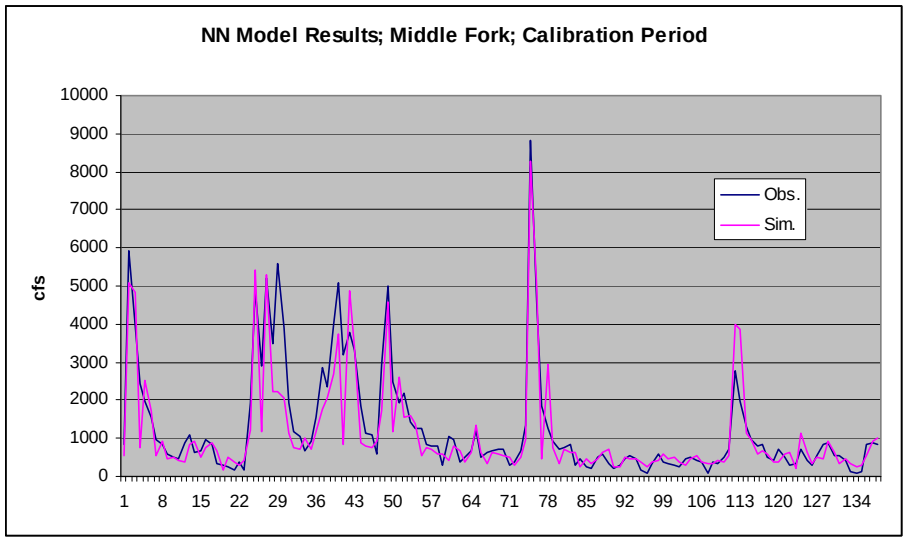

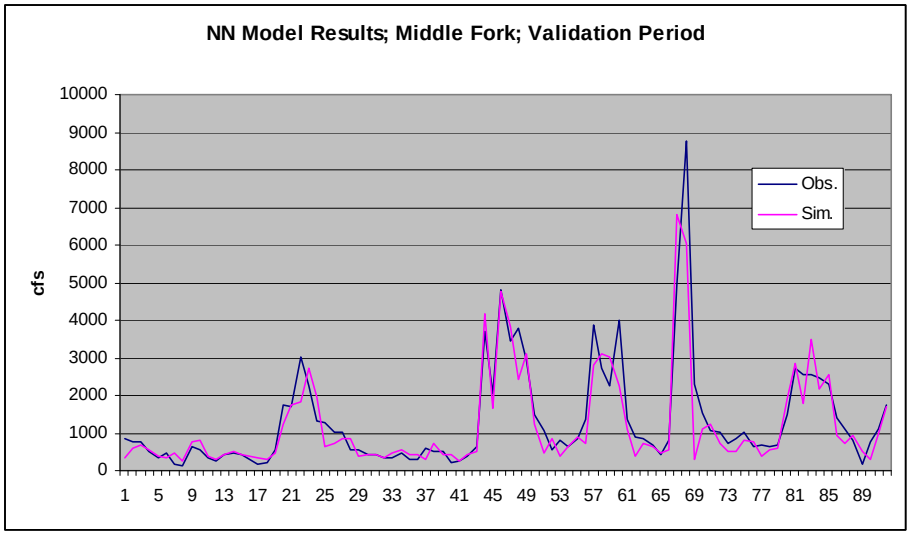

Figure B.10: Monthly NN Model Results; Middle Fork

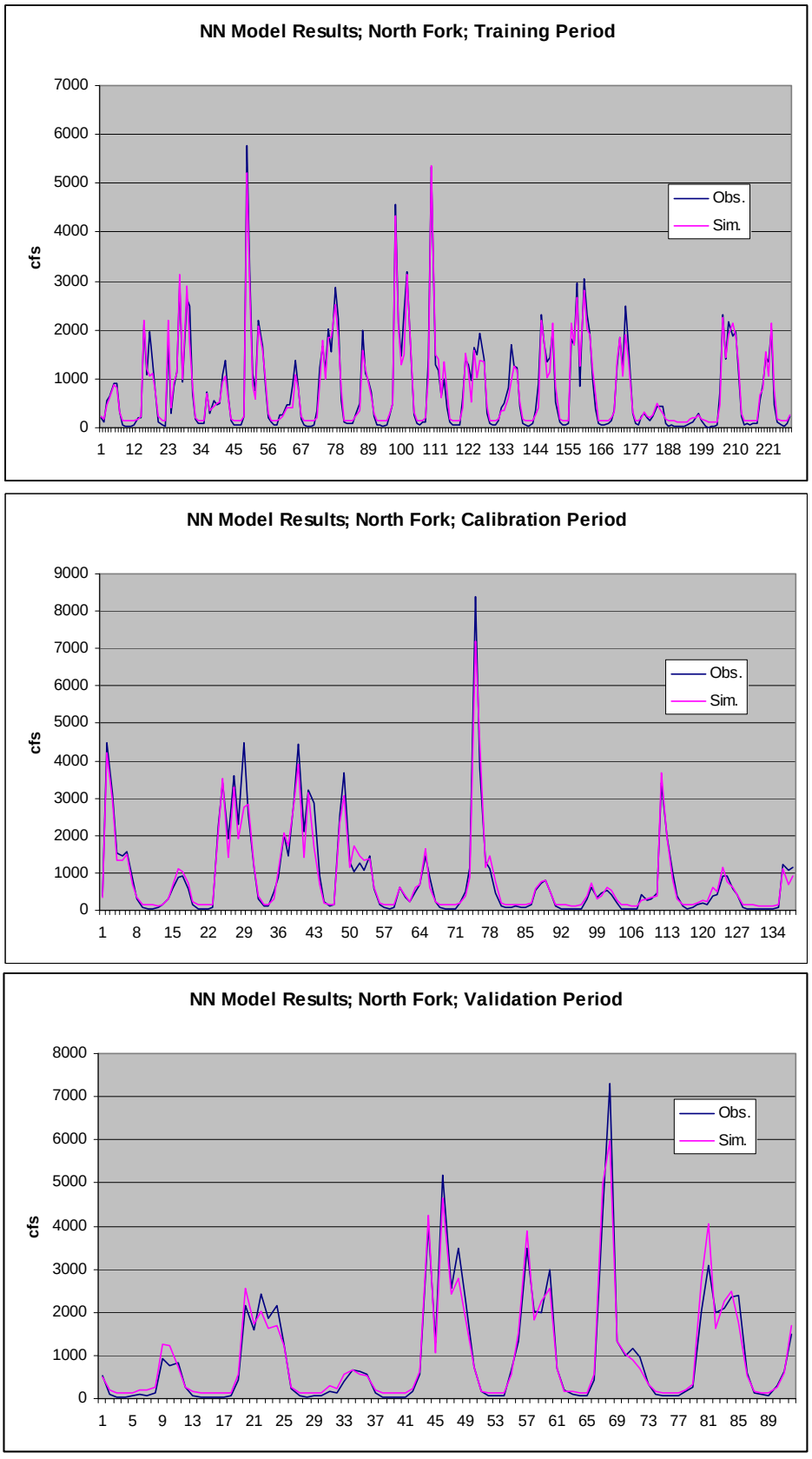

Figure B.11: Monthly NN Model Results; North Fork

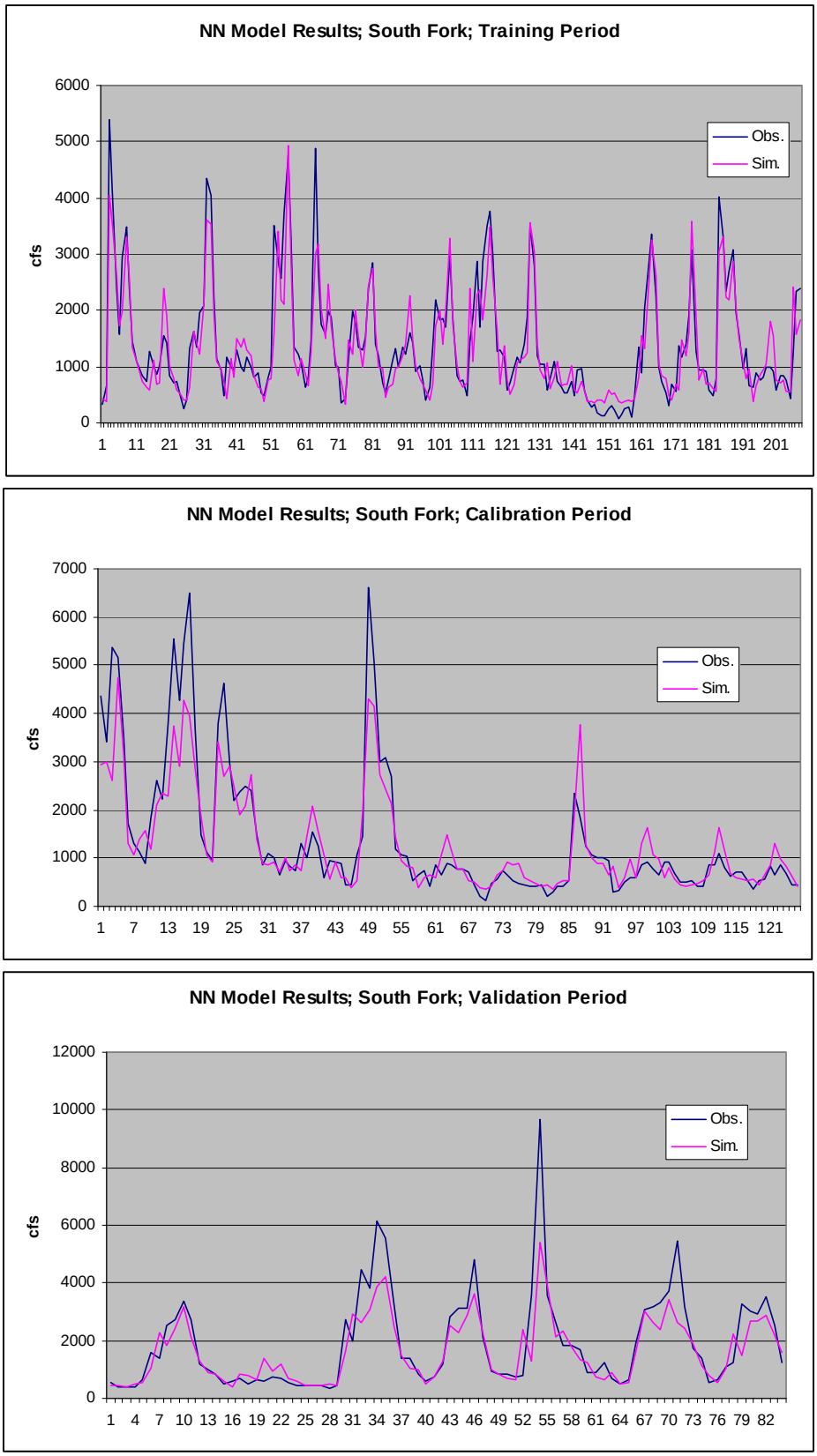

Figure B.12: Monthly NN Model Results; South Fork

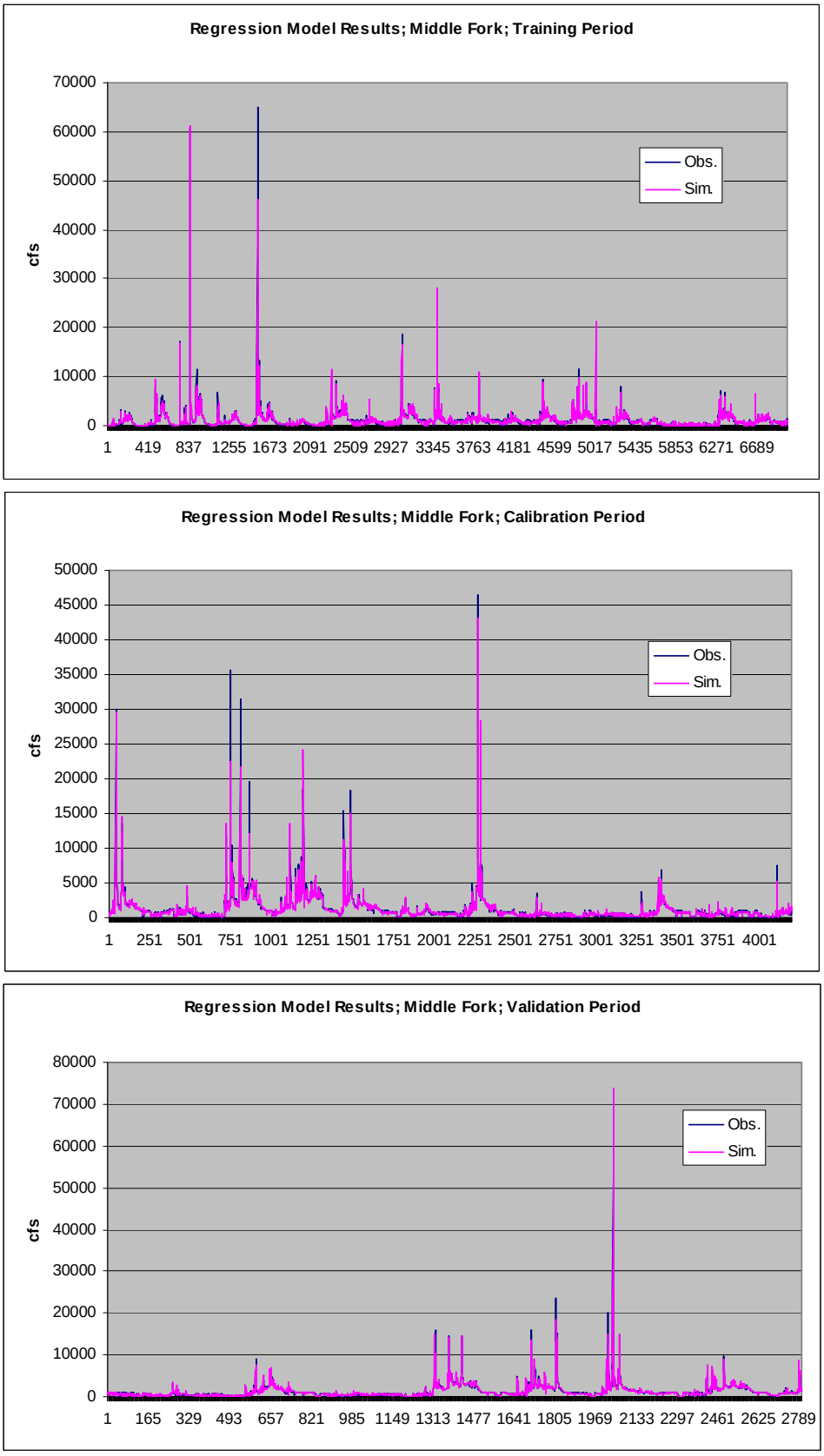

Figure B.13: Daily Regression Model Results; Middle Fork

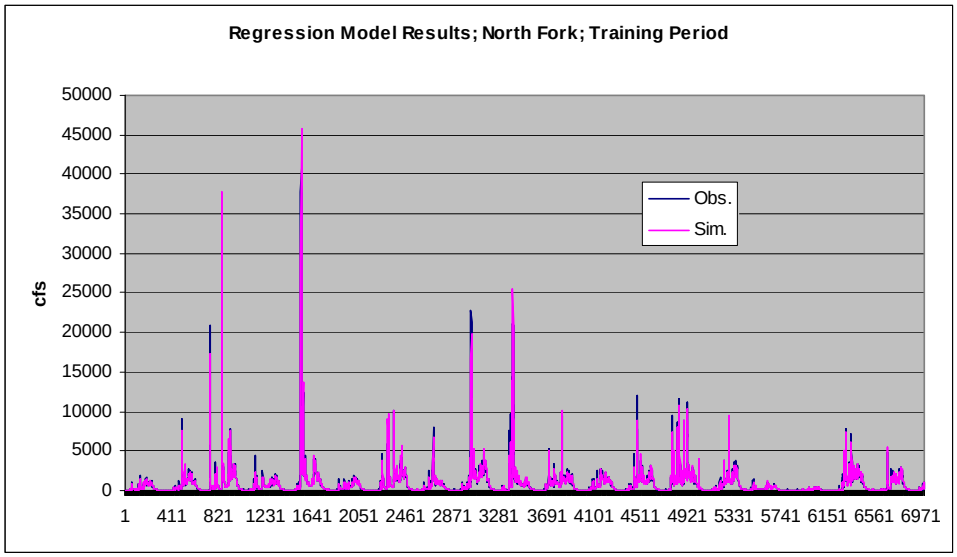

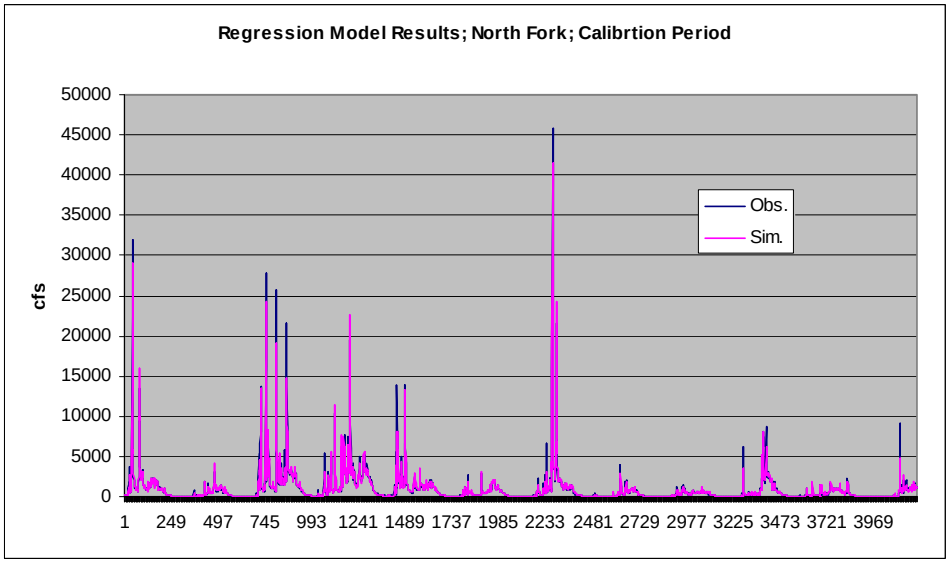

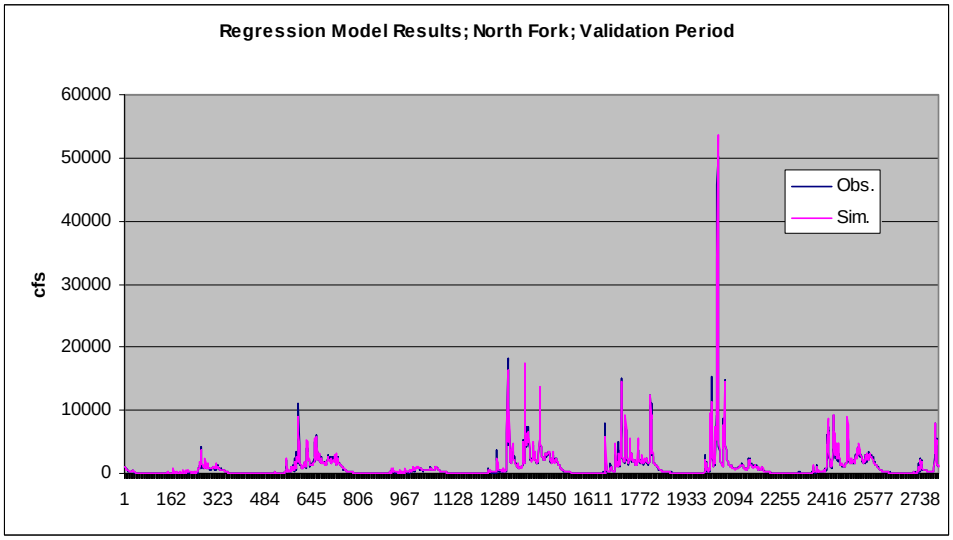

Figure B.14: Daily Regression Model Results; North Fork

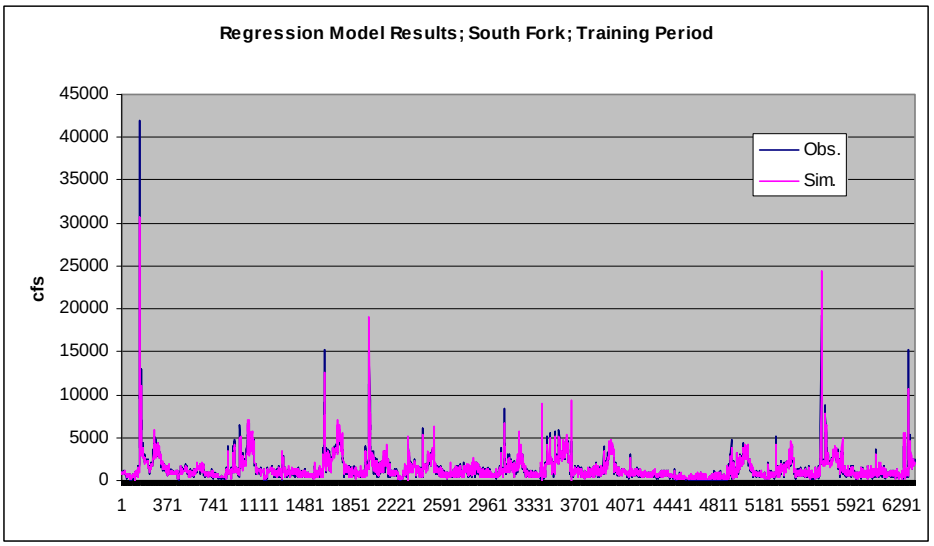

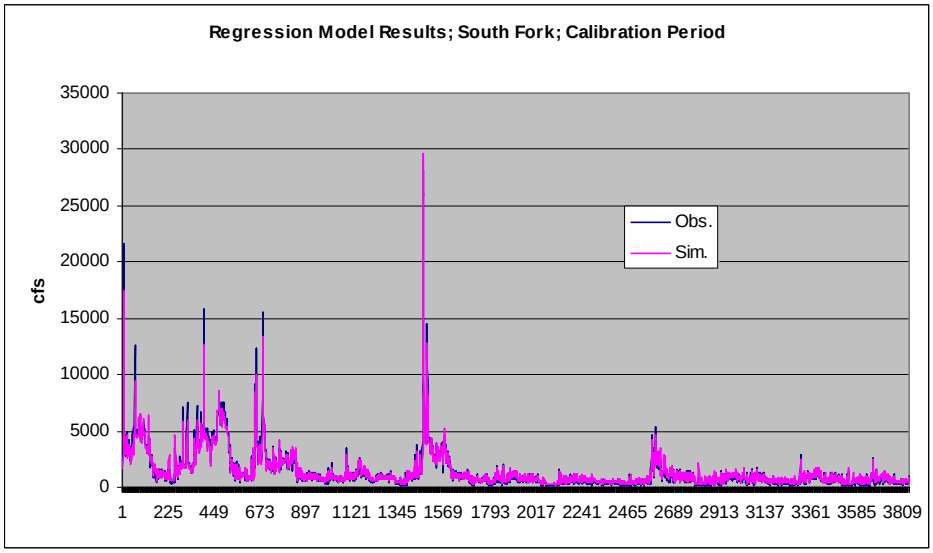

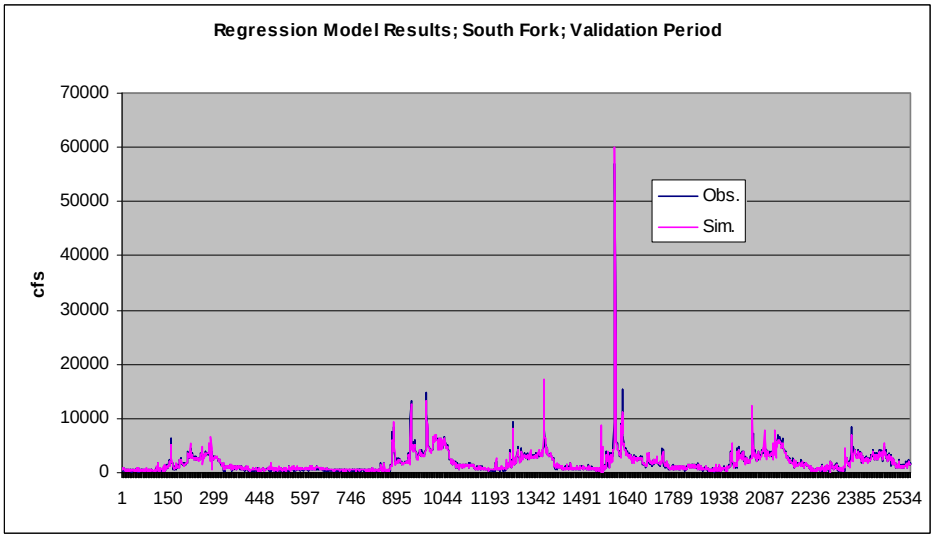

Figure B.15: Daily Regression Model Results; South Fork

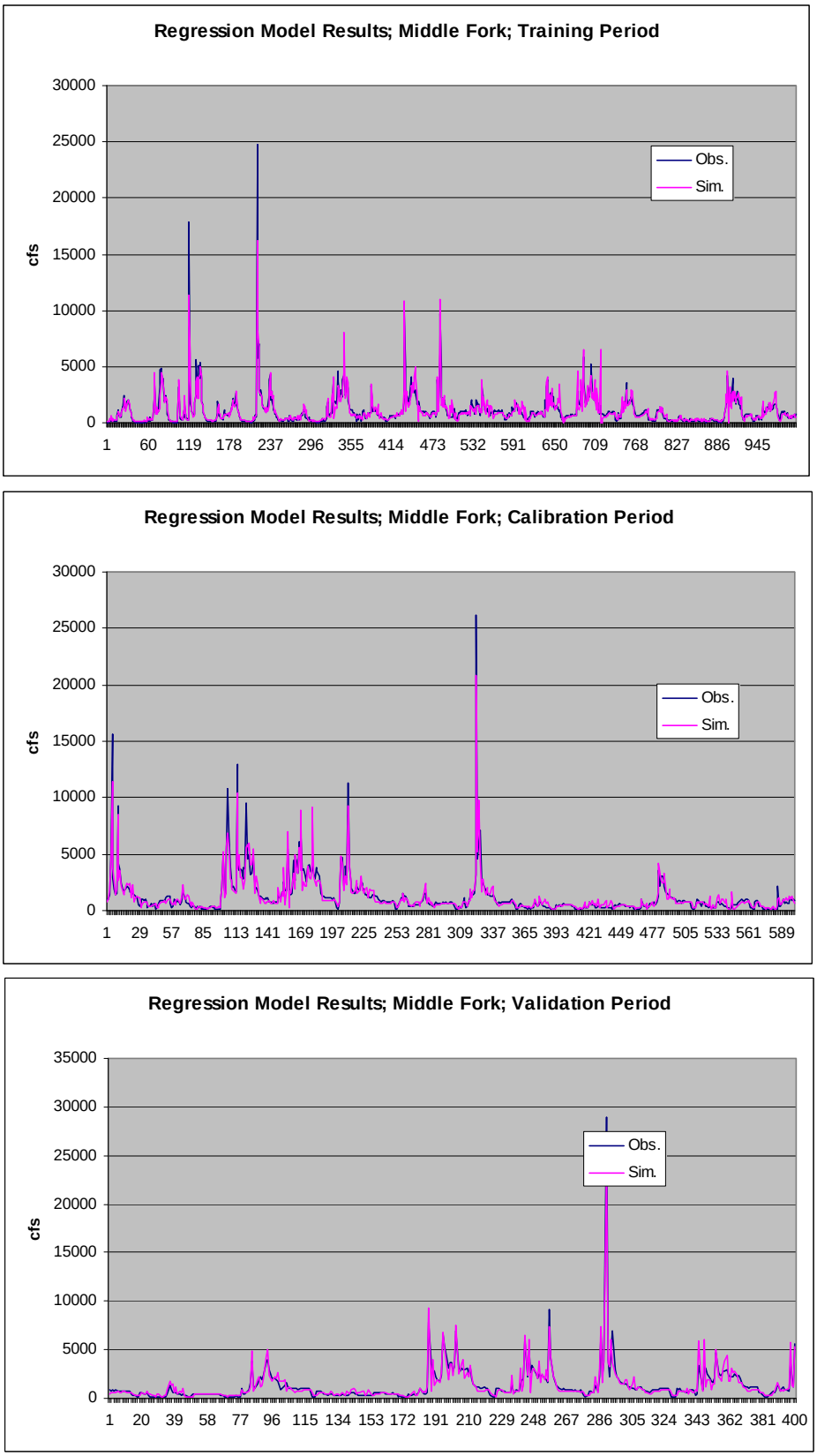

Figure B.16: Weekly Regression Model Results; Middle Fork

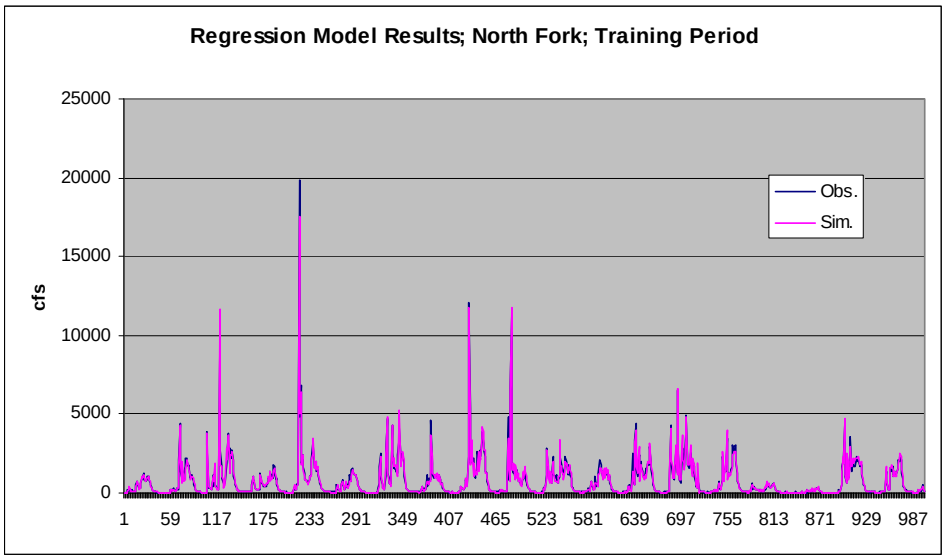

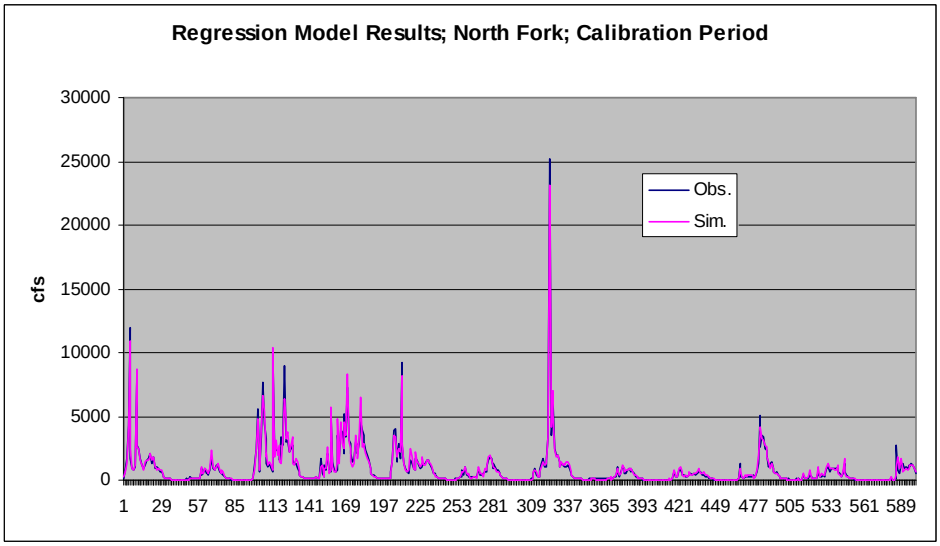

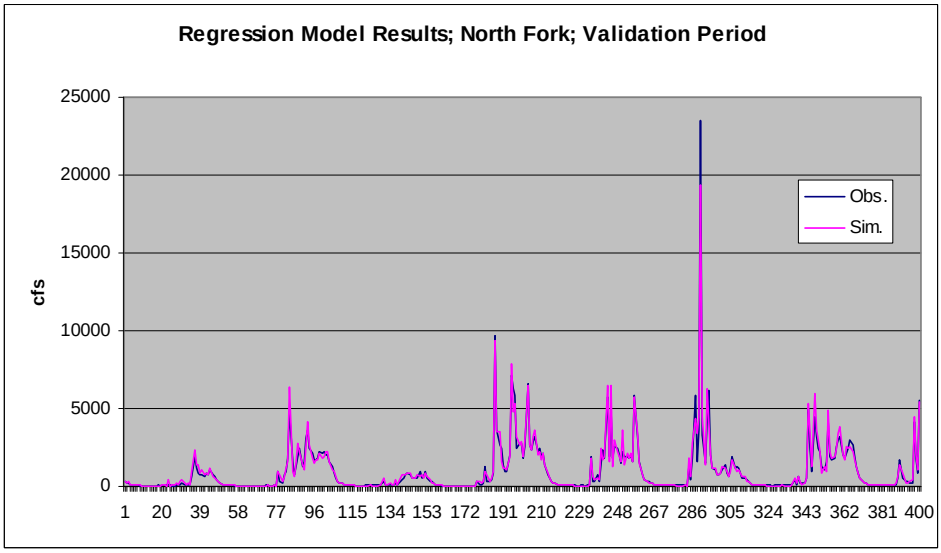

Figure B.17: Weekly Regression Model Results; North Fork

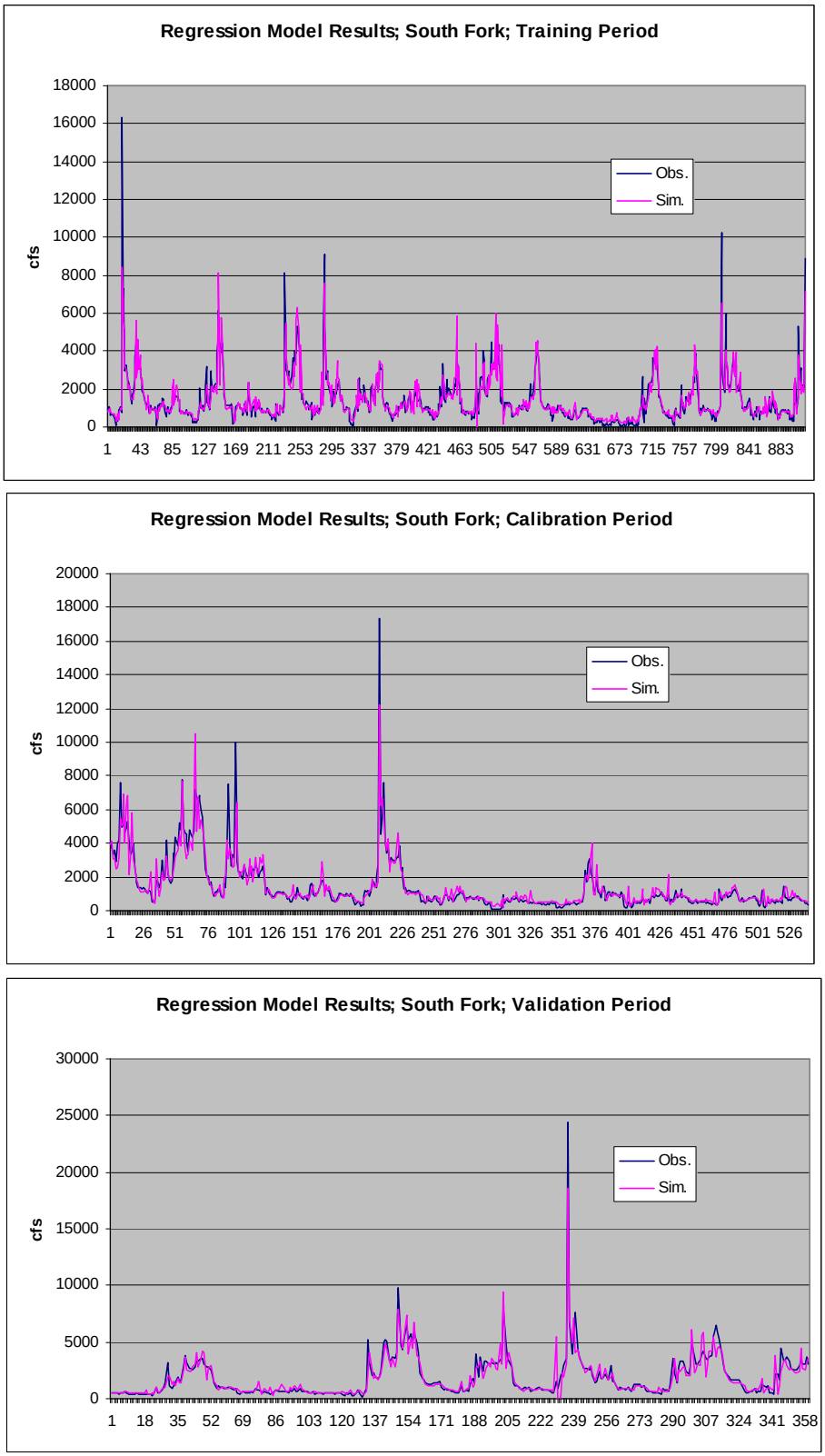

Figure B.18: Weekly Regression Model Results; South Fork

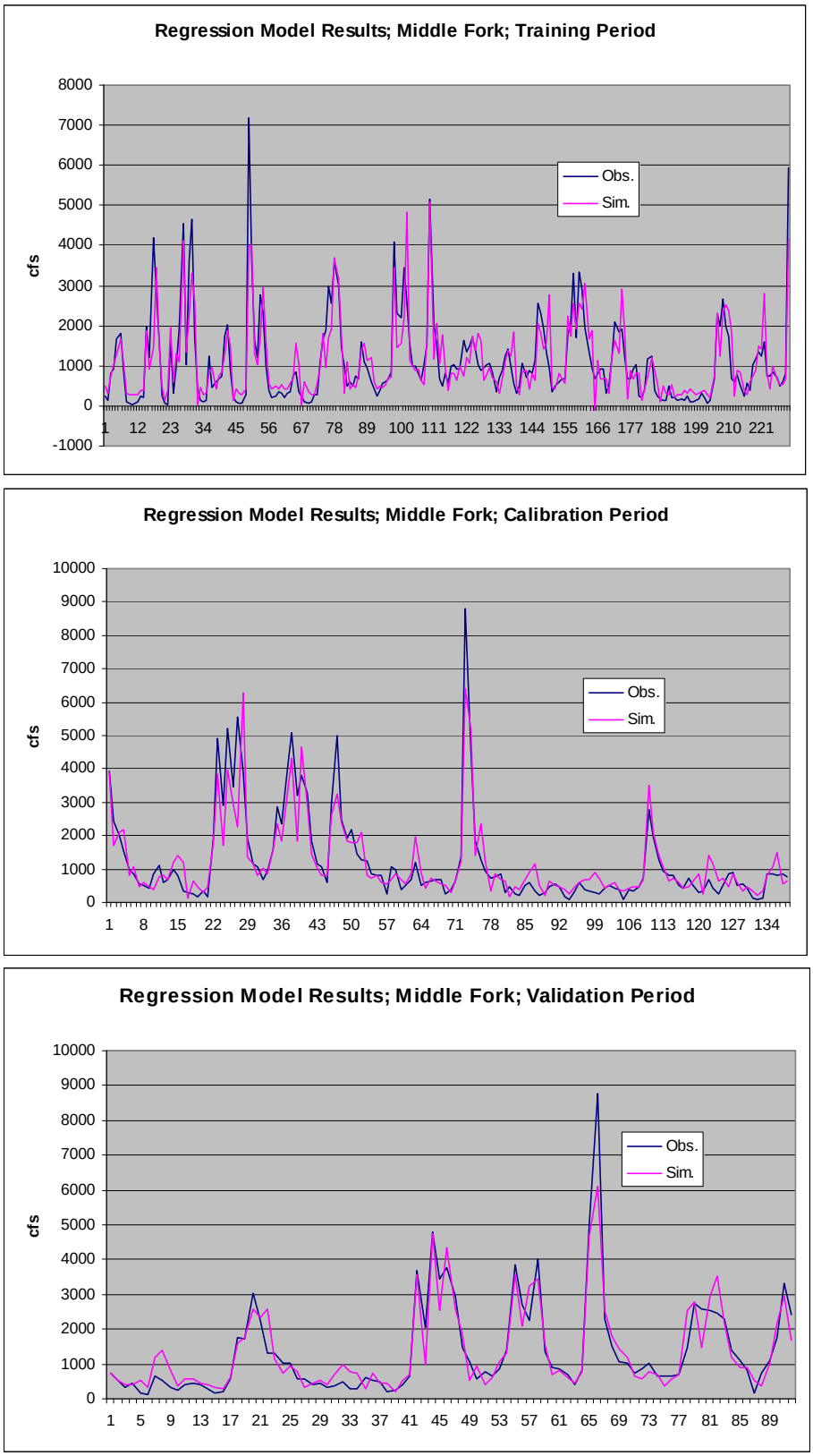

Figure B.19: Monthly Regression Model Results; Middle Fork

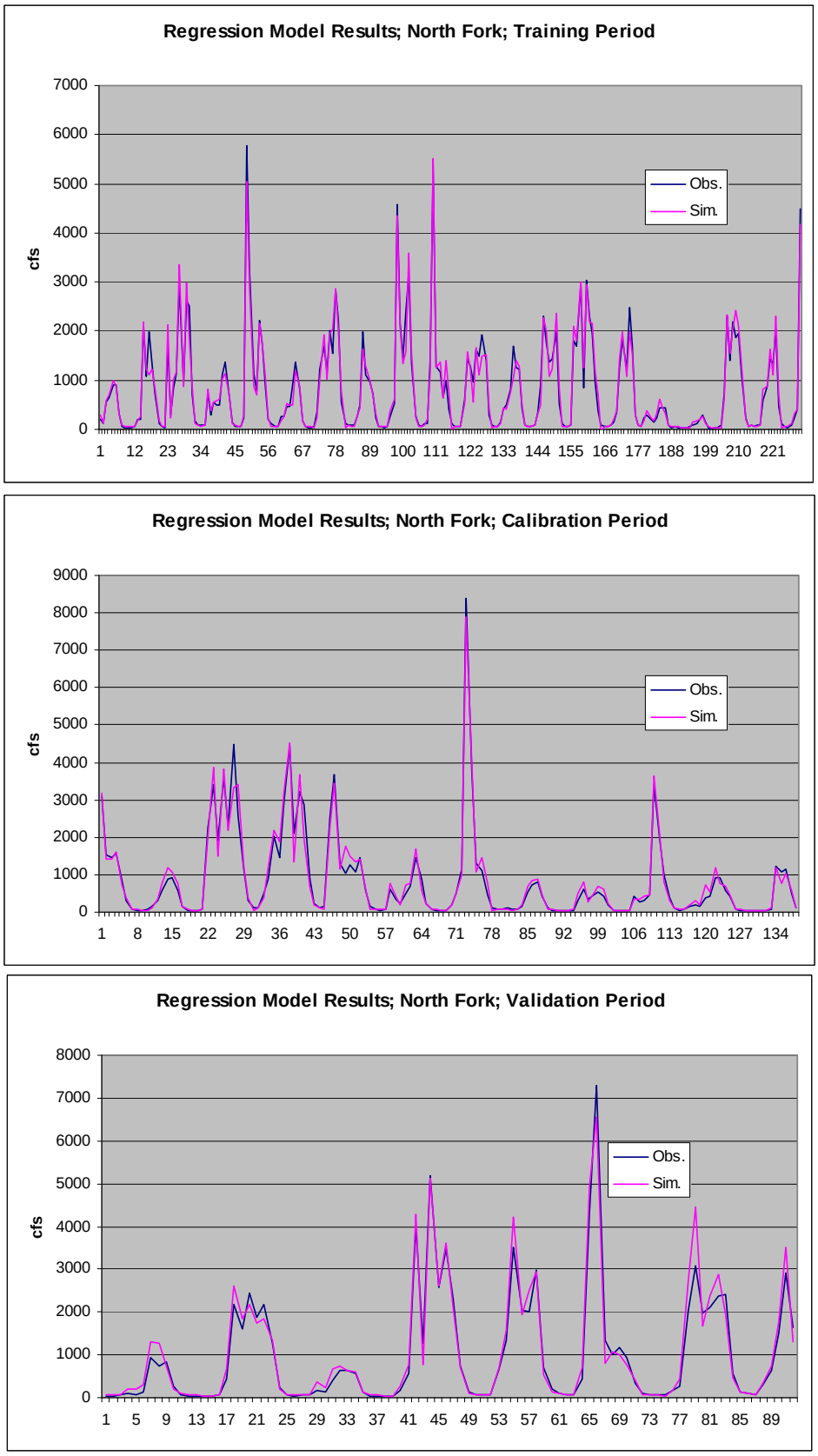

Figure B.20: Monthly Regression Model Results; North Fork

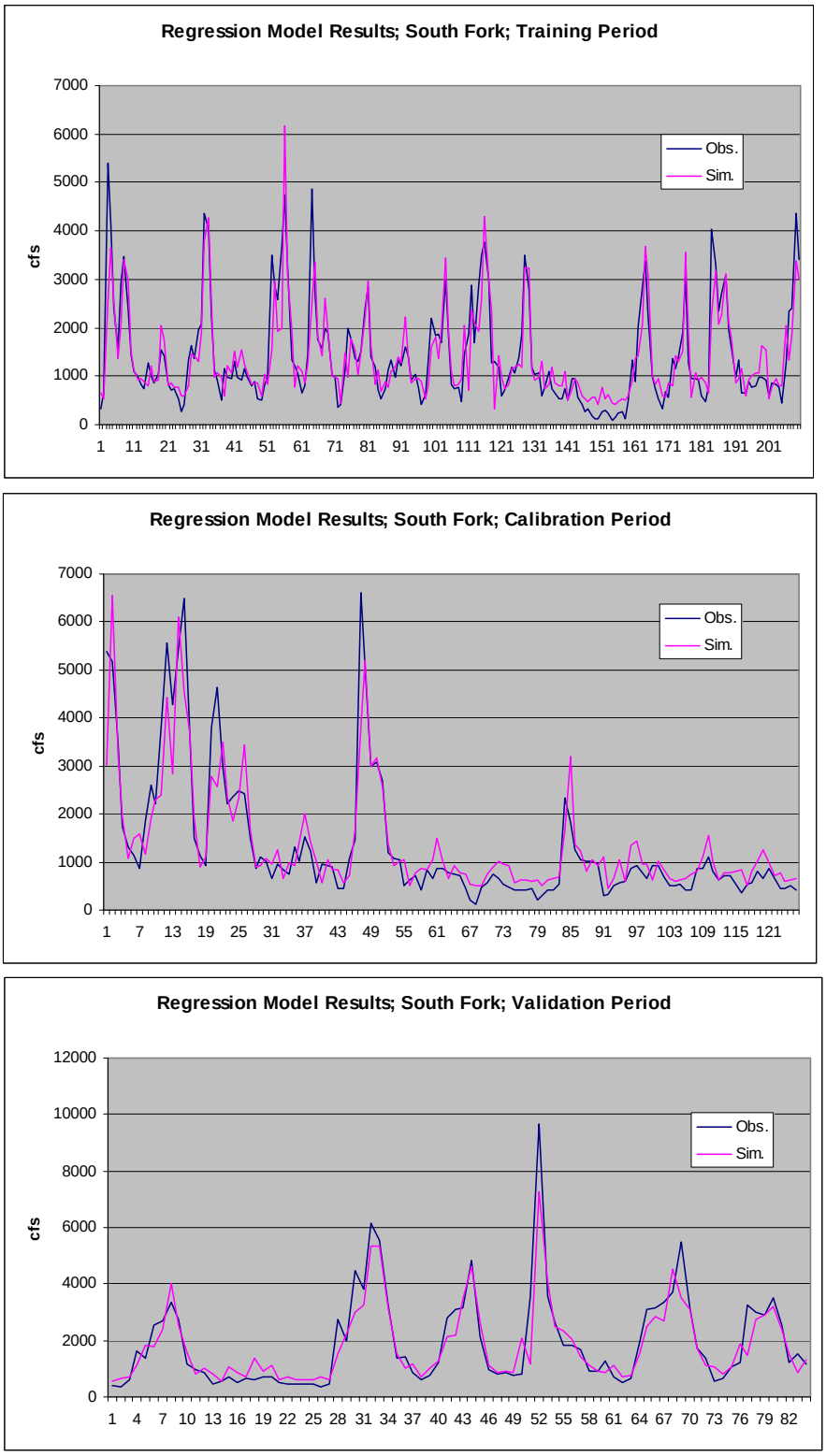

Figure B.21: Monthly Regression Model Results; South Fork

Appendix C: Performance Comparison by Frequency Range

C.1 Training Data Set

Table C.1: Performance Statistics for the Training Data Set (Middle Fork)

		Error Mean (cfs)	Error StD (cfs)	Correlation Coef
Lower Quartile	**Hydro Model**	-155.74	373.64	0.48
	Regression	-90.60	124.17	0.62
	NN	-72.13	77.58	0.58
Middle Half	**Hydro Model**	-22.12	884.28	0.16
	Regression	8.60	229.86	0.71
	NN	-54.25	177.88	0.76
Upper Quartile	**Hydro Model**	-85.30	1915.08	0.80
	Regression	95.26	1244.38	0.92
	NN	183.22	849.17	0.96

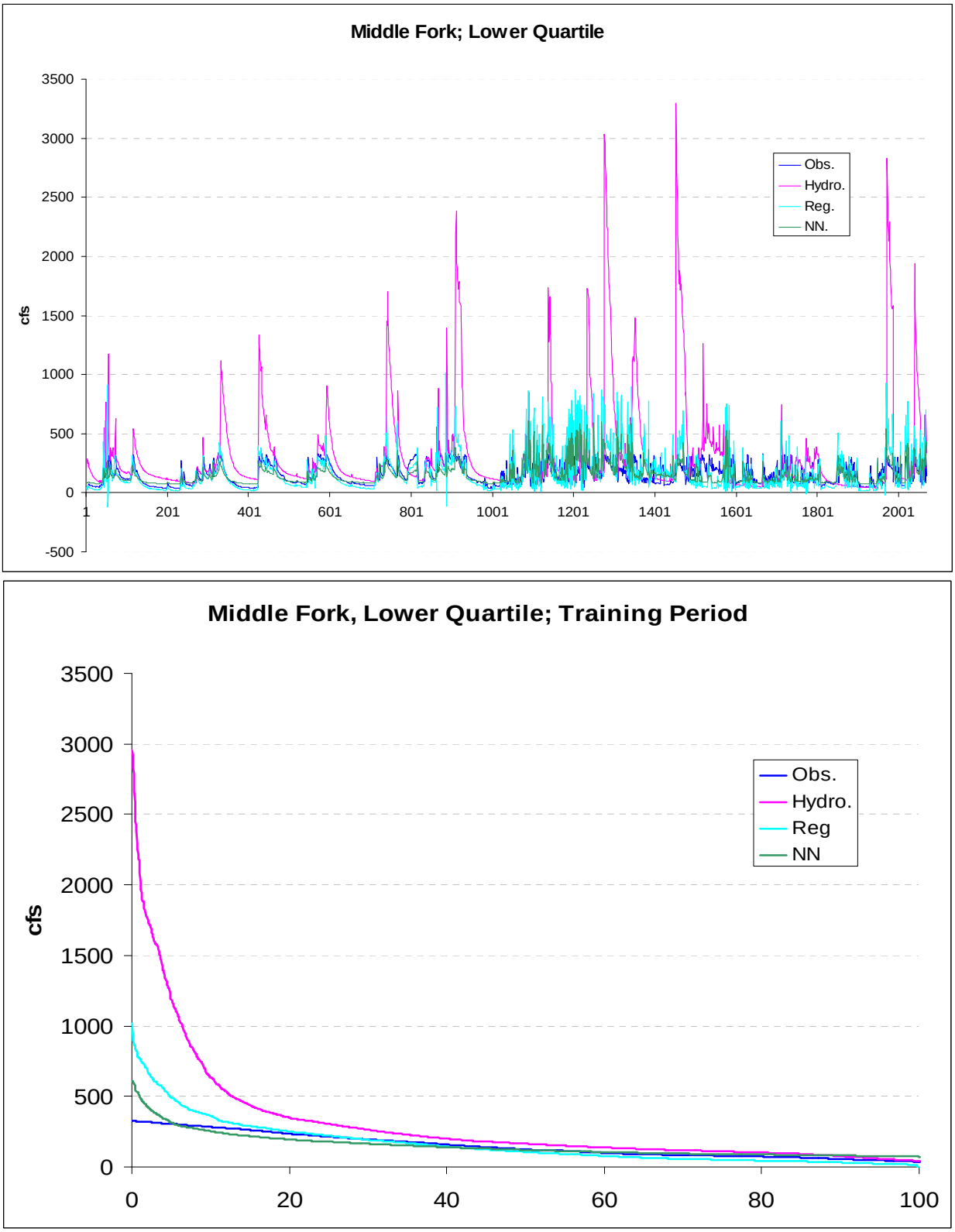

Figure C.1.1: Lower Quartile Training Data Set Comparison

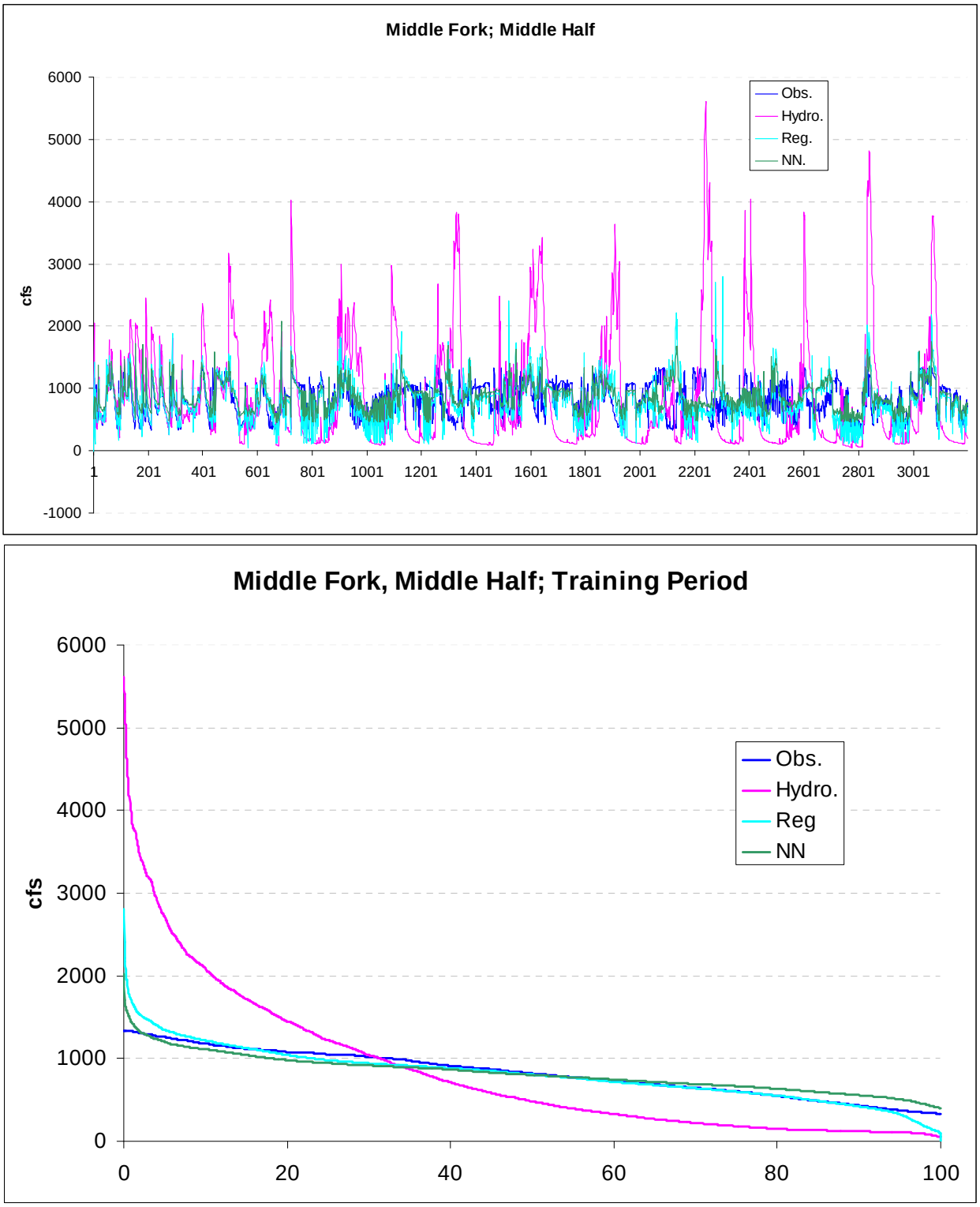

Figure C.1.2: Middle Half Training Data Set Comparison

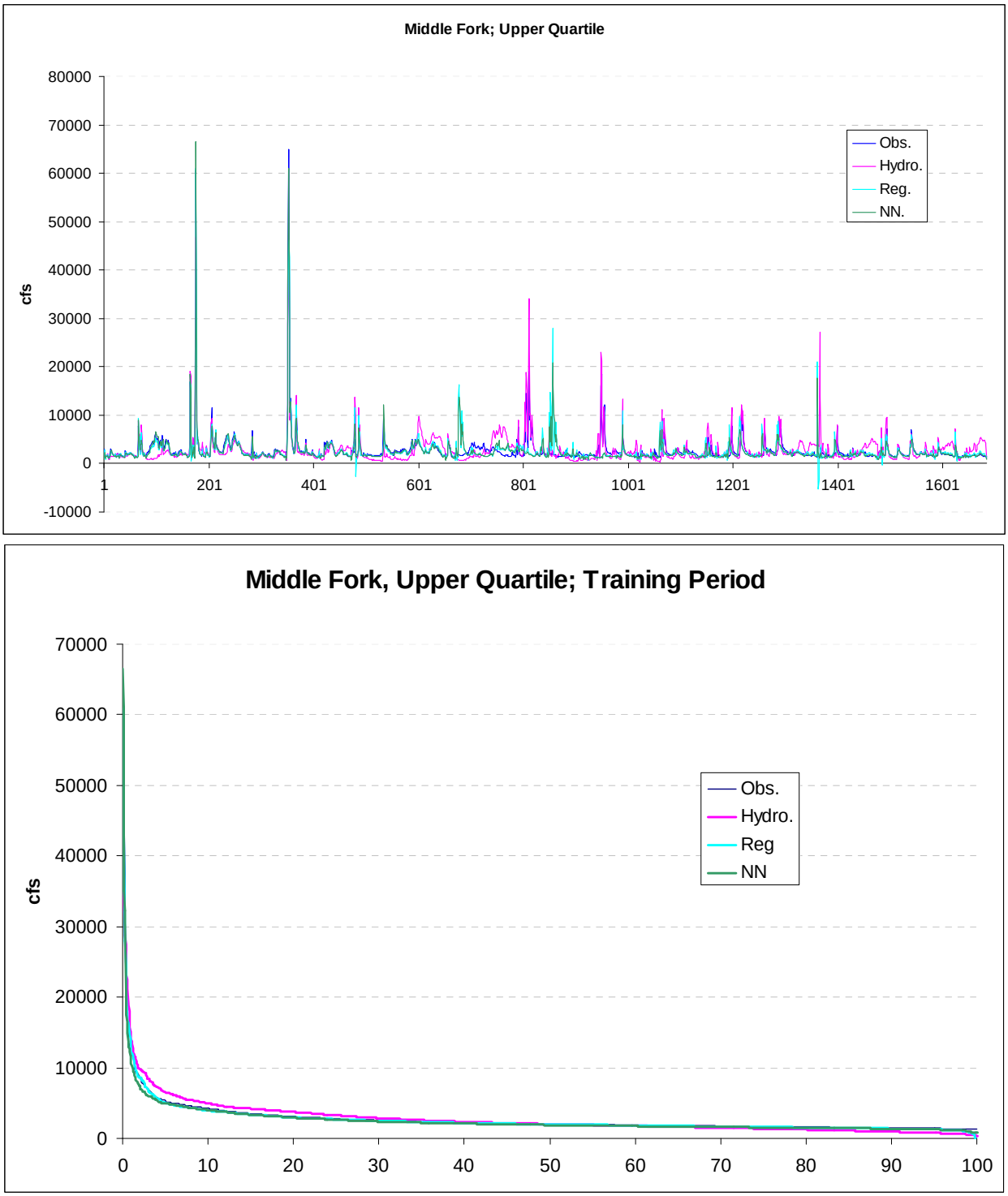

Figure C.1.3: Upper Quartile Training Data Set Comparison

C.2 Calibration Data Set

Table C.2: Performance Statistics for the Calibration Data Set (Middle Fork)

		Error Mean (cfs)	Error StD (cfs)	Correlation Coef
Lower Quartile	**Hydro Model**	-245.42	472.80	0.46
	Regression	-110.70	138.86	0.57
	NN	-61.32	80.73	0.56
Middle Half	**Hydro Model**	83.42	690.04	0.28
	Regression	21.07	194.89	0.76
	NN	-61.50	153.52	0.79
Upper Quartile	**Hydro Model**	-85.30	1915.08	0.80
	Regression	101.76	1110.68	0.95
	NN	248.18	1507.09	0.91

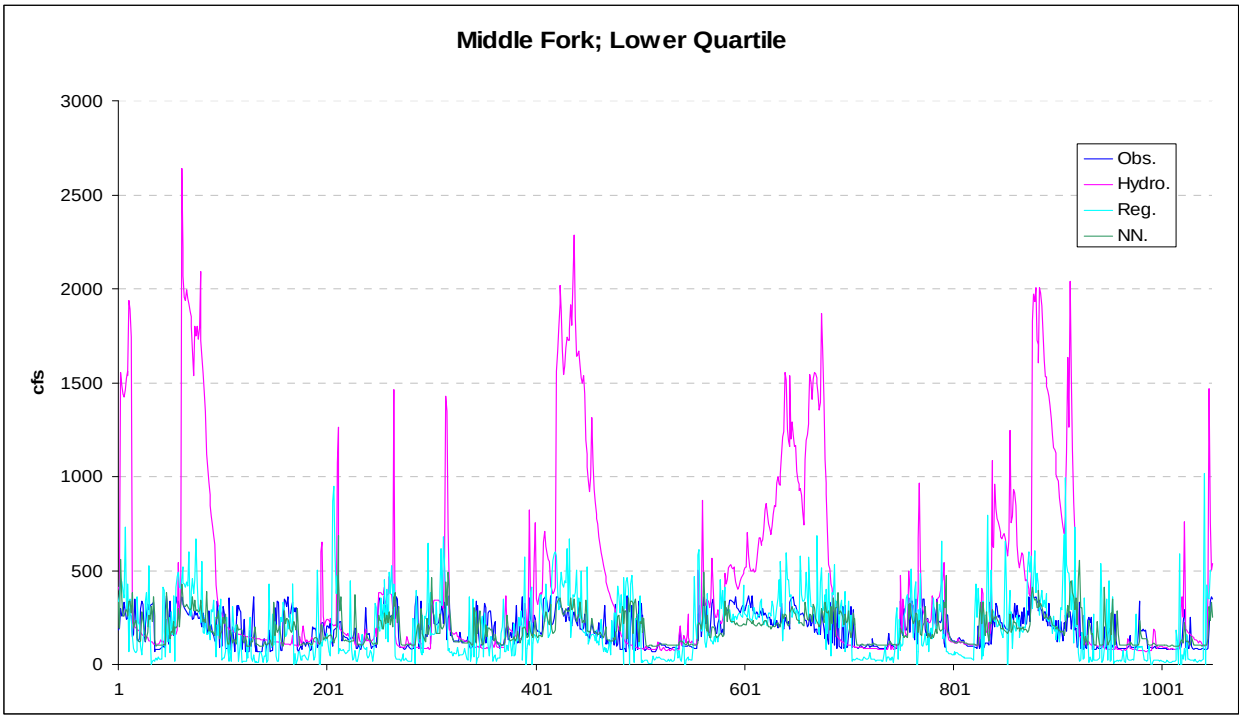

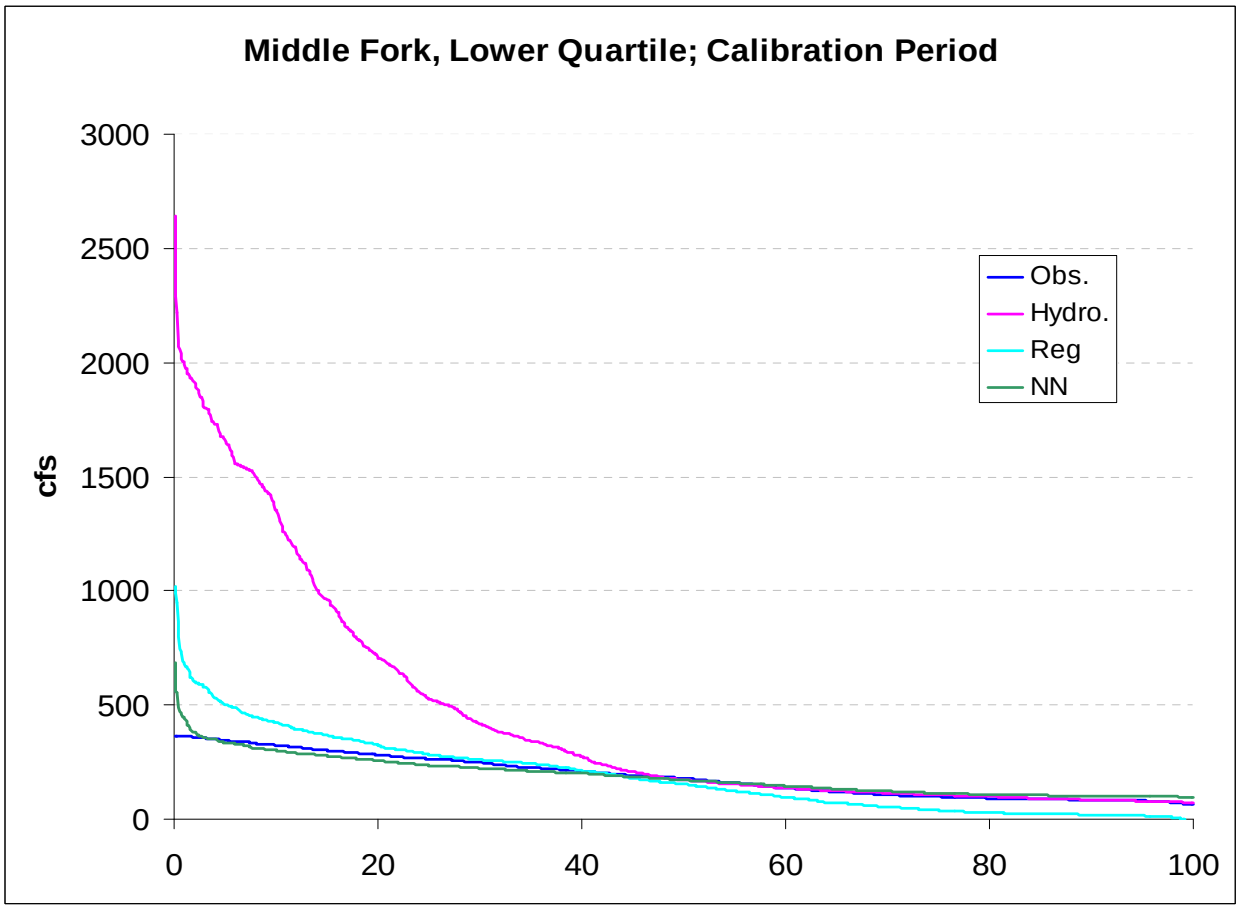

Figure C.2.1: Lower Quartile Calibration Data Set Comparison

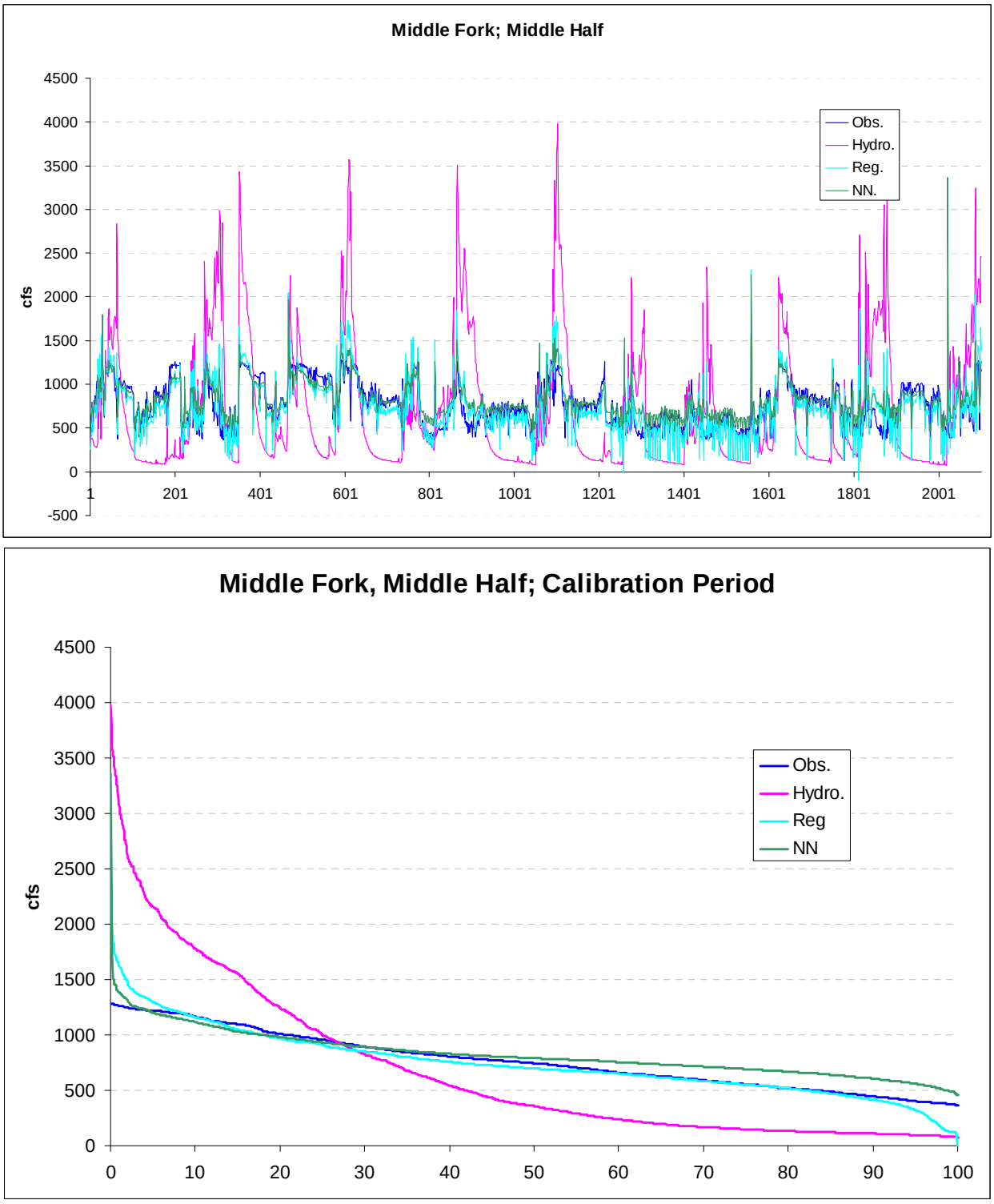

Figure C.2.2: Middle Half Calibration Data Set Comparison

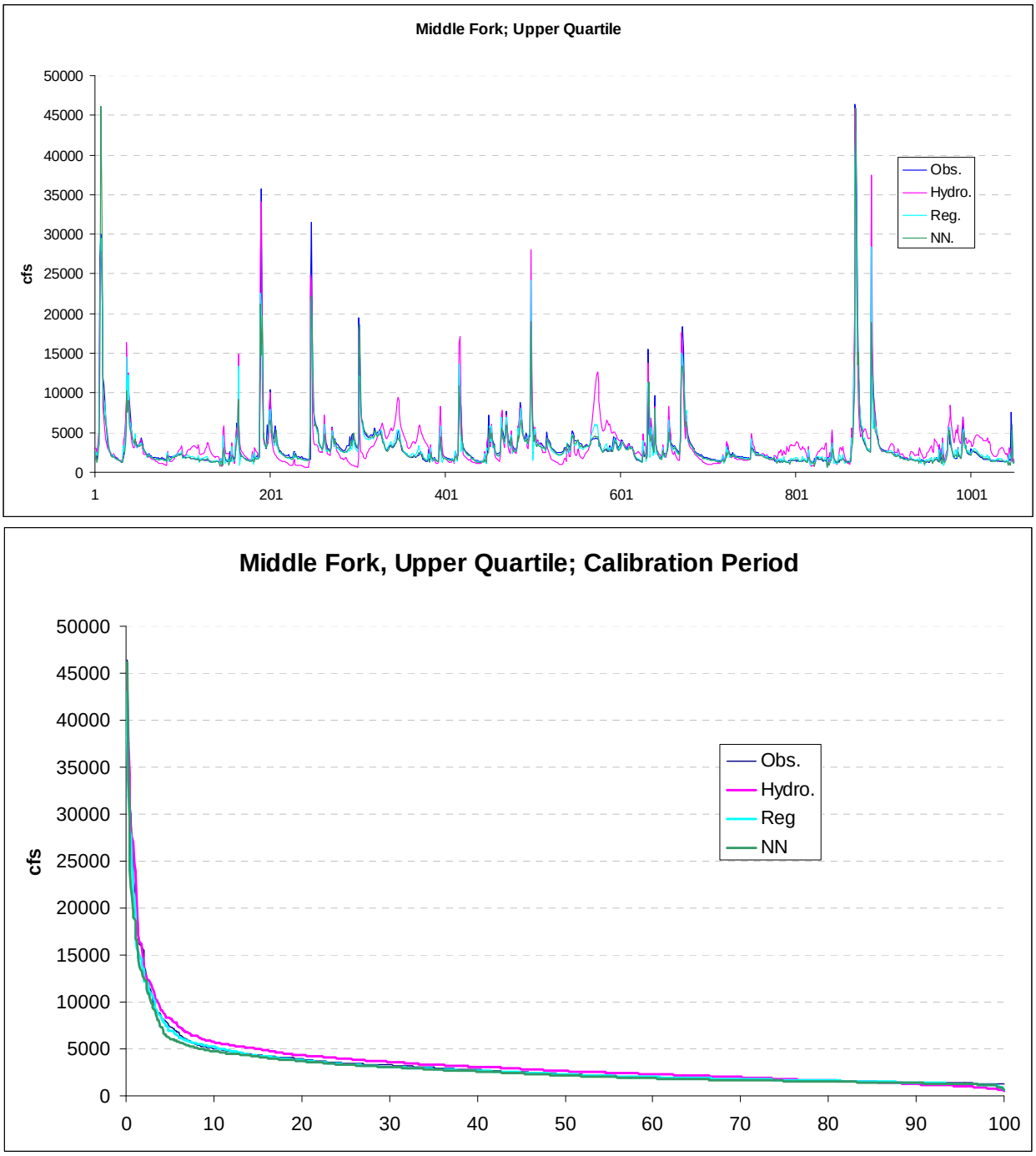

Figure C.2.3: Upper Quartile Calibration Data Set Comparison

C.3 Validation Data Set

Table C.3: Performance Statistics for the Validation Data Set (Middle Fork)

		Error Mean (cfs)	Error StD (cfs)	Correlation Coef
Lower Quartile	**Hydro Model**	-204.35	433.70	0.41
	Regression	-120.93	176.97	0.49
	NN	-57.75	113.21	0.49
Middle Half	**Hydro Model**	119.64	584.48	0.46
	Regression	44.74	234.03	0.75
	NN	-24.11	147.44	0.84
Upper Quartile	**Hydro Model**	-826.70	1564.62	0.92
	Regression	11.62	1194.29	0.95
	NN	302.47	1210.72	0.96

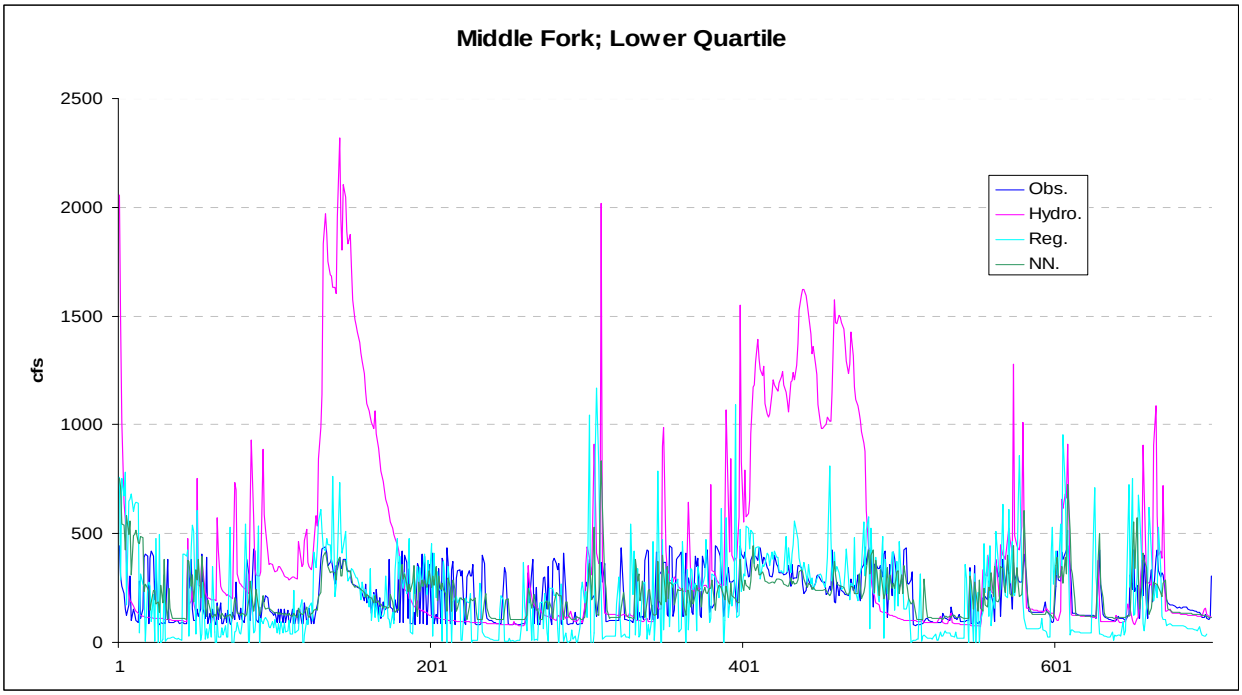

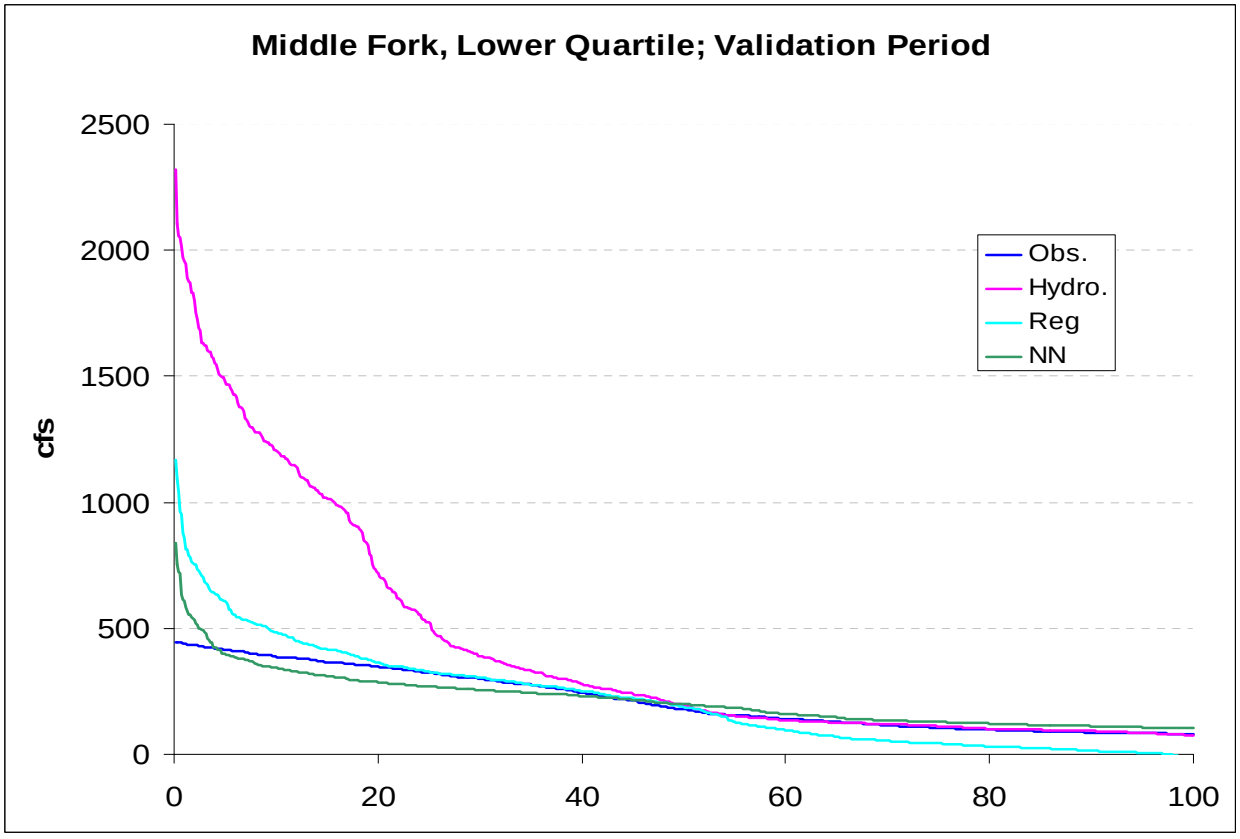

Figure C.3.1: Lower Quartile Validation Data Set Comparison

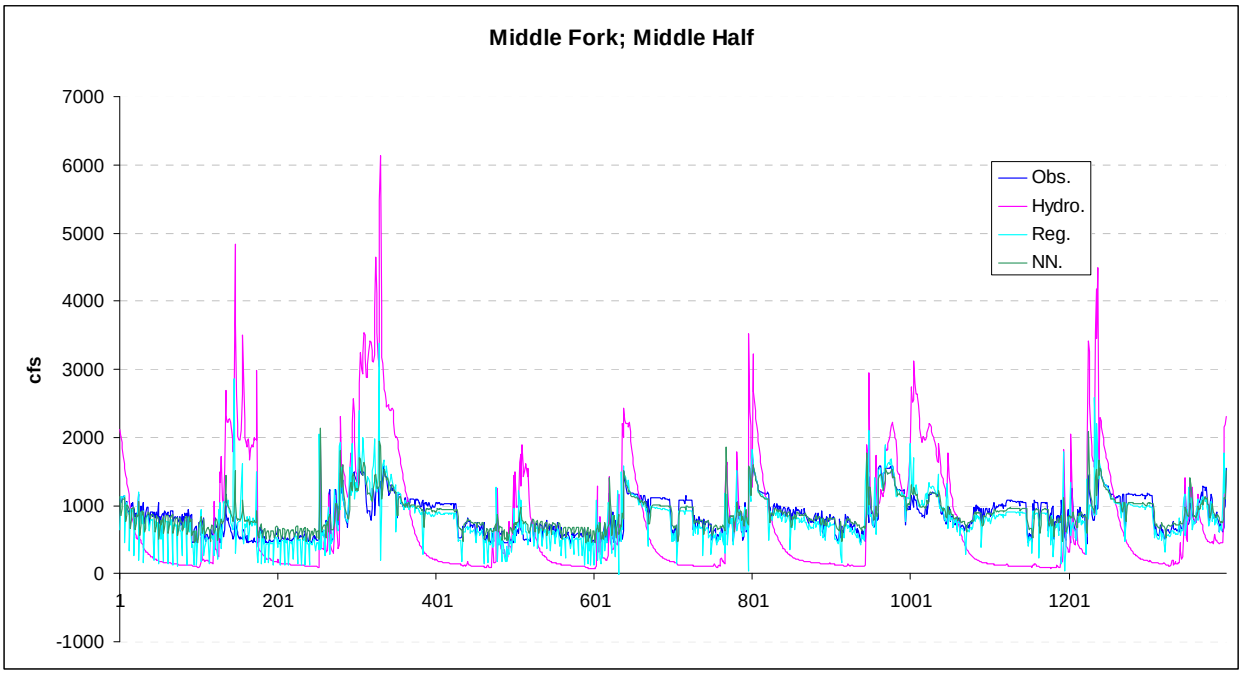

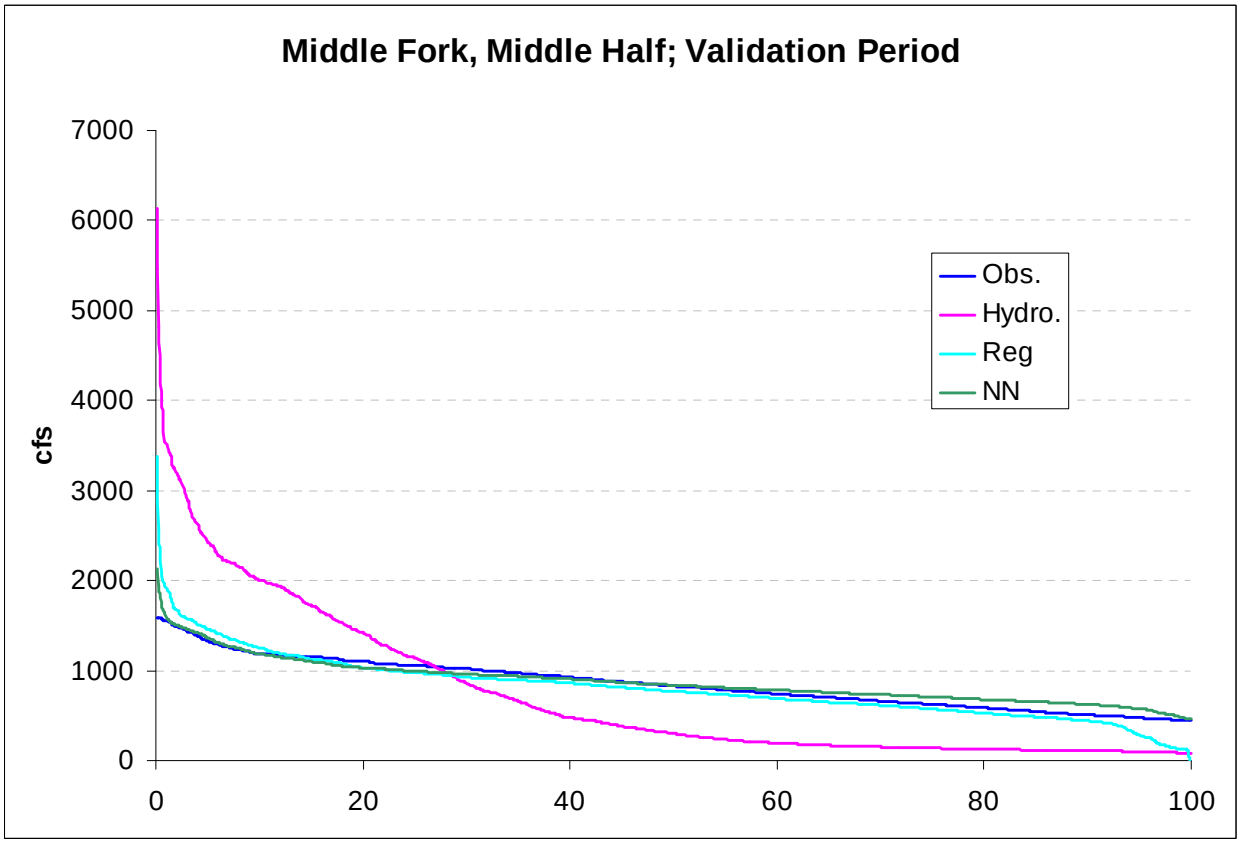

Figure C.3.2: Middle Half Validation Data Set Comparison

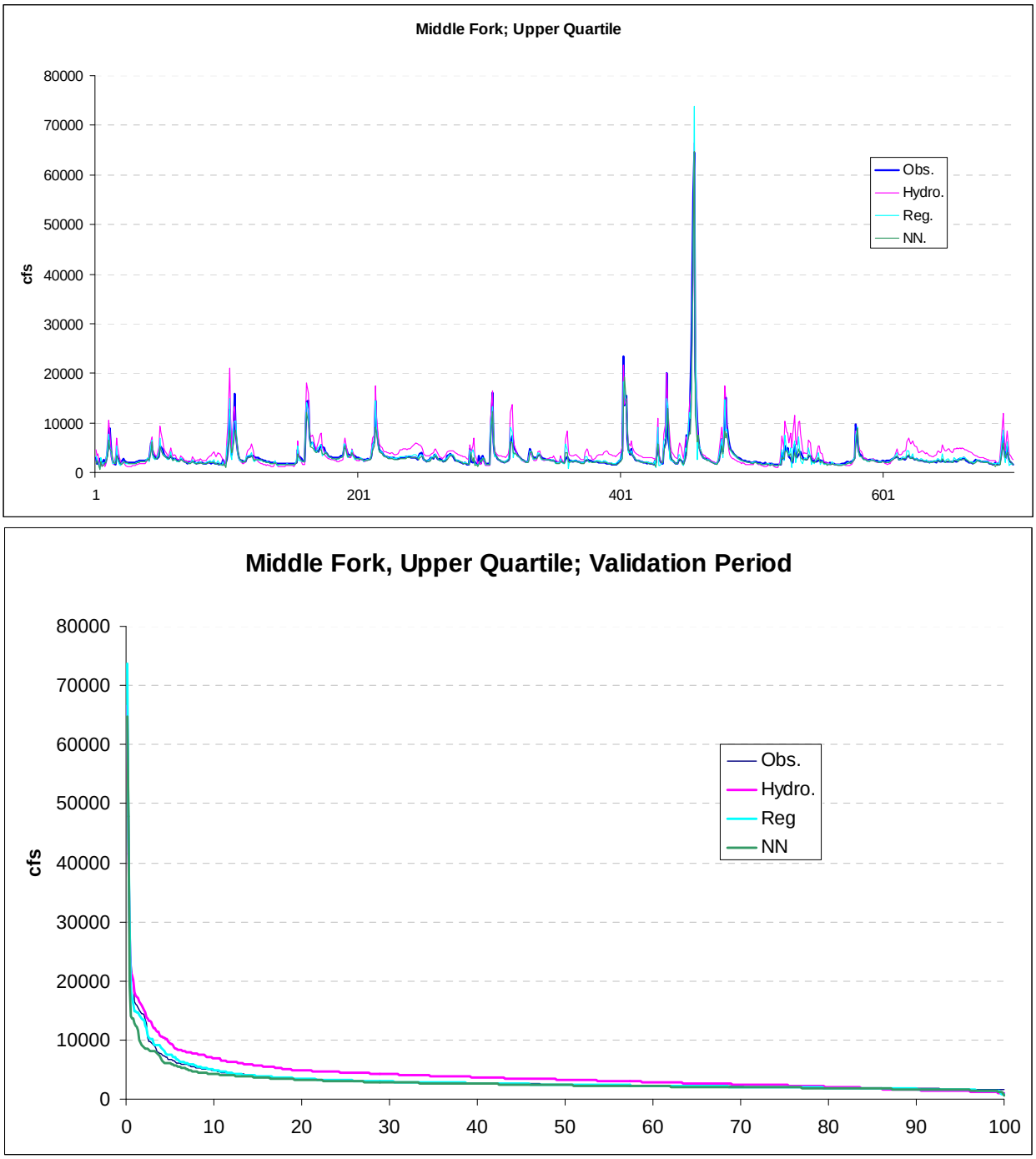

Figure C.3.3: Upper Quartile Validation Data Set Comparison